DESIGN STUDIES FOR STAND OFF BOMB DETECTION

by

CHRISTOPHER P. MATTHEW

B.S., United States Military Academy, 2000

A THESIS

submitted in partial fulfillment of the requirements for the degree

MASTER OF SCIENCE

Department of Mechanical and Nuclear Engineering
College of Engineering

KANSAS STATE UNIVERSITY
Manhattan, Kansas

2010

Approved by:

Major Professor
Dr. William Dunn

Copyright

Abstract

A prototype system for detecting explosives at standoff distances, using a signature based radiation scanning approach, is being developed at Kansas State University. The prototype will incorporate both a machine x-ray source and a machine neutron source to generate signatures from unknown samples of material. These signatures can be compared to templates measured or calculated from known explosive samples using a figure-of-merit. The machine neutron source uses the fusion of deuterium and tritium to create 14.1 MeV neutrons. Due to its radioactivity, the tritium must be sealed within the system. A new method of controlling the gas pressure with the DT generator was developed using a Zr-V-Fe getter supplied by a commercial firm. The shielding and collimation of the 14.1 MeV neutron source is accomplished using layers of steel, high-density polyethylene and borated high-density polyethylene. This thesis describes the development of the gas control method for the sealed neutron source, design studies for the shielding and collimation of the neutron source and modifications made to the building in which the prototype is being housed.

Table of Contents

List of Figures

List of Tables

Acknowledgements

I would like to thanks Dr. Bill Dunn for his mentorship and teaching over my two years at Kansas State University. I would like to thank Dr. Steve Eckels and Dr. J. Kenneth Shultis for their time and effort serving on my graduate committee. I would like to thank Adelphi Technologies for the opportunity to work with them and conduct research on the development of the DT-111 Neutron Generator. I would like to Hannes Vainionpaa for his help in learning about the Microwave Ion Source used for the DT-111. I would like to recognize Josh Burns for the countless hours that he has spent perfecting and revising the technical drawings of the prototype explosive detection system, many of which are presented here. I would like to thank M2 Technologies for their support of the Stand Off Bomb Detection project. Lastly I would like to thank Chris Henderson, Richard Yang, Mark Johl and the rest of the S.O.B.S. for their companionship and assistance in learning the SBRS method and developing the lab prototype.

Dedication

To my brothers and sisters in uniform serving on the frontiers of freedom. It is my sincerest hope that this technology will someday help protect these brave men and women from those that would do them harm.

CHAPTER 1 - The IED Problem

In many parts of the world today, improvised explosive devices (IEDs) are a very real threat to military and law enforcement personnel as well as to the civilian populace. Improvised explosive devices are used to harass military and law enforcement personnel and to cause fear among civilians. In many cases, they are used as weapons of assassination to kill political figures or local leaders. Figure 1.1 shows the total number of US fatalities in Iraq from March 2003 through July 2007. The line above the total shows the percentage of those fatalities that were caused by IEDs. In Iraq and Afghanistan, IEDs are the leading cause of casualties for U.S. and allied forces. From March of 2003 to September of 2007, IEDs were responsible for 1503 U.S. Soldier fatalities, or 39.5% of all US fatalities in Operation Iraqi Freedom (OIF) (Campbell and O'Hanlon 2007). While there are numerous technologies available to protect people from IEDs, detection prior to detonation remains the best method of preventing casualties.

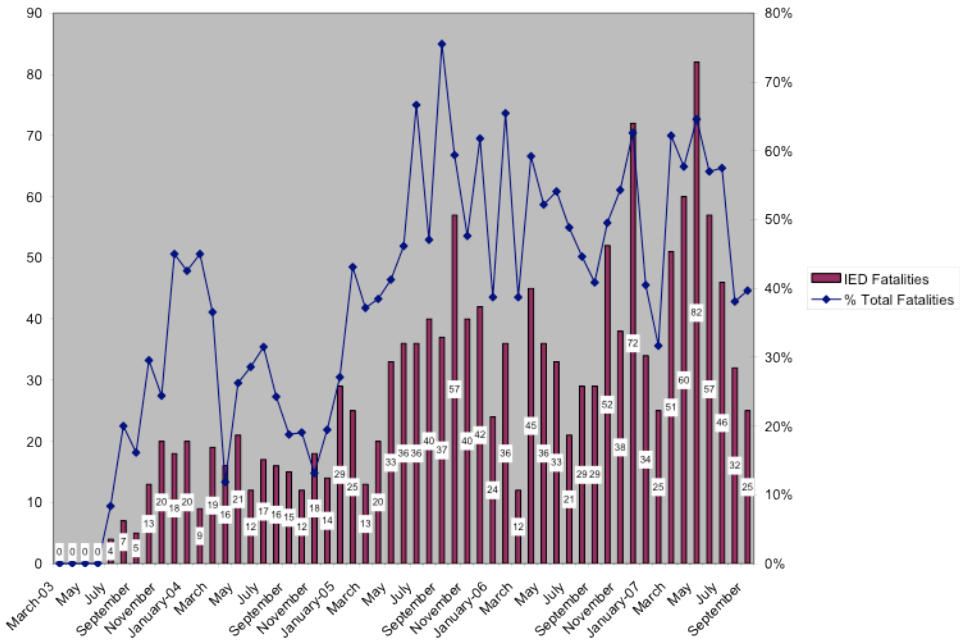

Figure 1.1 In this figure, the bars represent number of IED fatalities (left scale), by month, among U.S. forces. The line above shows the percentage (right scale) of total fatalities that were caused by IEDs

1.1 Categorizing Improvised Explosive Devises

There are many different types of IEDs employed against US forces. IEDs are primarily differentiated by the type of explosive used and the method of triggering the detonation. Most IEDs are simple devices consisting of a bulk explosive and an electronic trigger of some kind. The explosives are either home-made, such as those made of ammonium nitrate, or military grade munitions. A popular military explosive used for IED construction is the 155 mm artillery shell. Ammonium nitrate, which can be made using fertilizer, is also widely used in the production of IEDs. Whether an IED is constructed from military grade munitions or home-made chemical explosives, it must be triggered in some way.

Triggers for IEDs are typically electronic and can be made from a number of devices. They can be either active, requiring someone to trigger the device, or passive, in which case the device is triggered automatically when some condition is met. In some cases the trigger is as crude as touching contact wires to a car battery to complete a circuit. These simple triggers cannot be defeated by electronic countermeasures, but are not particularly threatening because they must be manually triggered from a point close to the explosive. There are other active triggers, such as cell phones, long-range cordless phones or short-range transmitters such as an electric doorbell or garage door opener, which can be activated from a distance. These devices are fairly simple and can be defeated using electronic countermeasures. Other triggers are passive in design. These include pressure-plates, trip-wires, crush-wires and infrared devices. One of the most widely used passive triggers is a passive infrared receiver (PIR). These are commercially available and are used as motion sensors in home security systems. When the heat of a passing vehicle is detected by the PIR, it will trigger the explosive. These devices are particularly dangerous because they are easily concealed and not easily defeated.□□

A particularly deadly variety of IED is what is known as an explosively formed projectile (EFP). These devices are composed of a steel tube packed with explosives, typically ammonium nitrate, and a copper plate. The explosive force of the ammonium nitrate forces the copper plate into a molten slug, which can penetrate deep into armor plating on a vehicle. These devices are deadly because they are usually deployed in combination with a PIR trigger. The lethality of the device combined with the difficult-to-defeat trigger make EFPs a serious threat to military and law enforcement personnel.

1.2 Current Method of Protecting Personnel from IEDs

Currently, there are many ways that military personnel protect themselves from the IED threat. Each is effective against a certain type of threat, but there is no one solution to protect from all types of IEDs. The protection methods include armor, electronic counter-measures, visual surveillance and pre-detonation scans.

1.2.1 Increasing Armor Protection

Increasing the level of armor on military vehicles provides protection against most common IED attacks. One example of this is the retrofitting of all High Mobility Multipurpose Wheeled Vehicles (HMMWVs) in Iraq and Afghanistan with what is called FRAG 5 armor. This increases the thickness and changes the composition of the armor plating in the doors of the vehicle as well as the underside and the roof. All glass in the vehicle is replaced with multi-pane ballistic glass. This provides increased protection from IEDs, but at the cost of mobility and maneuverability. These heavily armored vehicles are more prone to rollover during high speed maneuvering and also have a greater tendency to get stuck in loose terrain such as sand or mud. Even with this added armor, the HMMWV is still very vulnerable to EFP attacks.

1.2.2 Electronic Countermeasures

Many simple remote triggers can be defeated using electronic countermeasures. Every coalition patrol that leaves a forward operating base in Iraq is outfitted with at least one high power transmitter. This transmitter is set to send out a high power signal that scans through many of the frequencies used by remote triggers such as cell phones and long-range cordless telephones. This prevents the trigger from receiving the detonation signal. These jammers are effective against most, but not all active remote triggers, but cannot defeat hard-wired triggers or PIR devices. Another way to defeat remotely triggered IEDs is through a method known as pre-detonation. Here, an aircraft will overfly a specific area for a certain length of time and continuously broadcast commonly used detonation frequencies. This method is effective against IEDs using electronic doorbells, keyless entry remotes and other simple electric triggers. In some cases, it will cause a trigger to fire before the IED can be emplaced, rendering the device useless. However, as with electronic countermeasures, this technique does nothing to protect against PIR and other passive trigger IEDs.

1.3 Current Techniques for Detecting IEDs□□

While the combination of all of these techniques does provide a large degree of protection against IEDs, the best way to prevent loss of life is to detect the device before it is detonated. There are several methods employed throughout the world to detect and defeat explosives. (Hannum 1998) All of these share two crucial disadvantages; they are time consuming, and they require personnel to get close to potentially dangerous substances.□□

1.3.1 Trace Detection□□

One of the primary techniques currently used to detect explosives is trace detection. This technique requires the screening of targets for traces of explosive chemicals. This can be accomplished by wiping the sample with a small cloth that is then examined in a machine to determine if any traces of a number of dangerous substances were transferred from the sample to the wipe cloth. Another method for trace detection is the use of highly trained canines to smell a target. The dog is trained to react a certain way to let the handler know that it detects a certain scent. While highly effective, both of these techniques require trained personnel to be very close to the potential threat.□□

1.3.2 Visual Search□□

Another method employed by military and law enforcement personnel around the world is a visual search at a static checkpoint. These checkpoints are established around important areas or along major thoroughfares. Dependent upon the situation, every vehicle and person passing through this checkpoint may be stopped and inspected. A thorough inspection of a vehicle takes five to ten minutes. Also, the personnel conducting the inspection must receive specific training to ensure they know what to look for. Although this is primarily a visual means of identifying explosives, this technique has the same disadvantages as trace detection in that it requires personnel to work in close proximity to the threat.□□

1.3.3 Active Patrolling□□

Aside from static checkpoints designed to protect important areas, military and law enforcement also use patrols to try and keep critical supply routes clear of IEDs. These patrols are made up of highly trained personnel, using the best equipment available to search for IEDs along roads. They primarily use visual searching techniques, but also can employ some

mechanical means to detect potential threats. One example of a mechanical search is the use of the Meerkat or Husky mine detecting vehicle, shown in Figure 1.2. Both are used in a similar fashion. A single operator is protected in a blast resistant cabin and drives the vehicle over an area. Under the chassis is a metal detector that will sound an alarm in the operator's cabin when large amounts of metal are detected beneath the surface of the road. The vehicle also has an on-board marking system, to mark suspicious areas for follow-on interrogation. □□

Figure 1.2 A Husky Mine Detection Vehicle (left) and a Buffalo MPV (right).

The Buffalo Mine Protected Vehicle, shown in Figure 1.2, is the primary platform for visual interrogation. The Buffalo is a large, six-wheel truck with a v-shaped hull design to direct any blast energy around the crew cabin. Attached to the front of the vehicle a hydraulic boom that can extend out from the vehicle. At the end of this boom are a clawed spade and a video camera that is connected to a monitor in the crew compartment. This allows the crew to closely inspect any suspicious items from a distance, keeping personnel out of harms way.□□

Route clearance patrols are very effective. By 2007, more than half of all IEDs in Iraq were found and cleared prior to detonation (Campbell and O'Hanlon 2007). However, with an average travel speed of around 10 kilometers per hour, these patrols are very time consuming. The slow pace makes them more susceptible to direct fire attacks. Even with the best equipment and training available, injuries in these patrols are frequent. The heavily armored vehicles used in route clearance missions protect personnel from the shrapnel and debris from explosions, but they are often very close to detonations, and have a high risk of concussive injuries. □□

1.3.4 Persistent Surveillance□□

Another method of detecting IEDs is the use of persistent and temporary surveillance. In 2006 and 2007, the US Army tested a program code-named Highlighter, using aerial surveillance to try and identify possible threats. An aircraft would fly over a designated route and photograph

key areas. After a set time interval, the aircraft would over-fly the same area, at the same altitude and again photograph the same locations. A computer algorithm would highlight differences in the two sets of photos. An intelligence analyst would review the highlighted areas and submit those that looked to be a threat to the ground forces. A route clearance patrol would check any highlighted areas as soon as possible. There were several disadvantages to this and similar programs. For one, it still requires personnel to get close to the threat in order to verify it. Also, municipal services in Iraq are not as well developed as they are in the US, so trash tends to gather on the side of major roads. The trash already on the road being moved by the wind, as well as new trash being added caused problems in the identification of changes in the terrain.□□

1.4 The Need for Stand Off Bomb Detection□□

The combination of all of the previously mentioned protection and identification techniques helps to mitigate the IED threat, but there are still several limitations. All of these techniques share two common weaknesses. Each is time consuming and requires personnel and equipment to get in close to potentially dangerous IEDs. In order to more quickly and effectively defeat IEDs, a technique must be developed that is both rapid and robust while keeping personnel out of harms way. Signature based radiation scanning (SBRS) is a new method that can provide rapid detection of explosive material with high sensitivity and specificity (Dunn et al 2007). □□The goal of the stand off bomb detection project at KSU is to develop a prototype system that provides this rapid and robust explosive detection. The project uses back-streaming radiation signatures from unknown samples and compares these to the signatures expected from known explosives, in order to determine whether the sample is inert or explosive. While high specificity, or limiting false positive readings, is important, the emphasis is placed on high sensitivity, or eliminating false negative readings.

CHAPTER 2 - The Signature Based Radiation Scanning Approach

The SBRS method (Lowery 2010) offers a potentially rapid and robust method for identifying explosive materials based on the back-streaming radiation measured when irradiating an unknown sample. The radiation signatures can be compared to those from targets containing known explosives to determine if a sample is explosive or inert, within some confidence interval. A figure-of-merit (FOM) is defined based on the difference between the signature of the unknown sample and a known template. The lower an unknown sample's figure-of-merit, the more likely it is to be an explosive.□□

2.1 Collecting Signatures□□

There are several radiation interactions that can be used in explosives detection. If a target is bombarded with photons, the backscattered photons can be measured. The backscatter spectrum can be divided into low energy (multiple scatter) and high energy (single scatter). The backscatter response is mainly a measure of density. Most nitrogen rich explosives, such as ammonium nitrate, have a similar density of around 1.7 g/cm^3. If an unknown sample has a density much lower than this, it can be ruled out as an explosive immediately. The third signature that can be collected from photon interrogation is measuring Photon Induced Positron Annihilation Radiation (PIPAR). PIPAR is indicative of the chemical composition of the sample. The probability of a PIPAR formation varies with Z(A+Z), where Z and A are the mass number and atomic number of the element being irradiated.□□

Neutron interrogation adds another four possible types of signatures to be used in template matching. The first is prompt neutron capture gamma radiation. This occurs when a neutron is captured by a nucleus, forming a heavier nucleus through the reaction $^{A}X(n,\gamma)^{A+1}X$. The heavier nucleus will be excited by the neutron capture and will de-excite by emission of a photon. This photon has a characteristic energy dependent upon the nucleus from which it was emitted, allowing identification of specific elements within the sample. Backscattered neutrons can be measured by both bare and cadmium covered neutron detectors, providing two additional signatures. Finally, gamma rays induced by inelastic neutron scatter provide the fourth type of neutron signature. □□

2.2 Using Signatures to Determine the Figure-of-Merit

One method of identifying explosives is through what is called template matching. In template matching, the radiation response signature collected from an unknown sample is compared to that of a known sample. In this procedure, the signatures can be from both photon and neutron interactions. The collected signatures are then used to create the figure-of-merit. The figure-of-merit is essentially a difference of squares formula used to compare the signature from unknown samples to those of known samples. If the N signatures collected from a sample are arranged into a vector **R** such that:

$$\mathbf{R} = (R_1, R_2, ..., R_N). \tag{2.2.1}$$

where R_i is the i^{th} response signature from the unknown sample. This vector can be compared to a vector **S** of the responses from a known explosive, similarly:

$$\mathbf{S} = (S_1, S_2, ..., S_N). \tag{2.2.2}$$

Then the figure-of-merit (FOM) is given by:

$$\varsigma_l = \frac{1}{N}\sum_{i=1}^{N} \alpha_i \frac{\left(\beta R_i - S_{li}\right)^2}{\beta^2\sigma^2\left(R_i\right) + \sigma^2\left(S_{li}\right)}. \tag{2.2.3}$$

Using the propagation of errors formula, the uncertainty of the figure-of-merit is determined by:

$$\sigma\left(\varsigma_l\right) = \frac{2}{N}\left[\sum_{i=1}^{N} \alpha_i^{\,2} \frac{\left(\beta R_i - S_{li}\right)^2}{\beta^2\sigma^2\left(R_i\right) + \sigma^2\left(S_{li}\right)}\right]^{1/2}. \tag{2.2.4}$$

2.3 Analyzing the Figure-of-Merit

Using the figure-of-merit and its uncertainty, a filter function can be defined as:

$$f_{\pm} = \varsigma_l \pm \lambda\sigma\left(\varsigma_l\right). \tag{2.3.1}$$

Here, λ is an adjustable parameter that determines the width of the confidence interval. The greater λ is, the more likely it is that the FOM lies within the interval. The value f is then tested against a predetermined cut-off value to determine if a sample is likely to be an explosive or not. If f_+ or the upper limit of the confidence interval is below the cutoff value, the sample is deemed to be explosive. If f_-, or the lower limit of the confidence interval, is above the cut of value, the sample is deemed to be inert. If the cut off value lies between f_- and f_+, then the test is inconclusive and further analysis is required. In practice, an inconclusive test would likely be

treated as an explosive sample until it was determined to be safe through further inspection. An example of this analysis is shown in Figure 2.1.

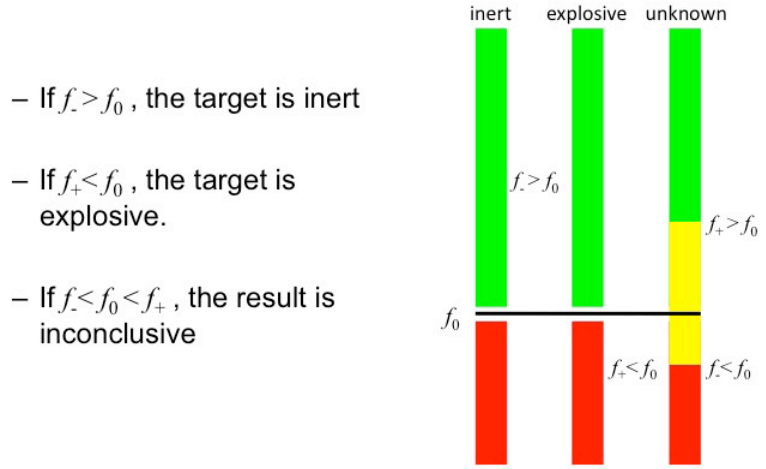

Figure 2.1 The figure-of-merit and filter function are compared to a specified cut off value to determine if the unknown sample is explosive, inert, or undetermined.

The cut-off value as well as the size of the confidence interval can be adjusted based on the situation. It is clear that a greater value of λ will reduce the value of f_-, thus reducing false negatives. However, this will also increase the value of f_+, which will increase the number of inconclusive tests. This essentially increases the number of false positives, because an inconclusive result is treated as an explosive. Similarly, decreasing the cut-off value will increase the number of false positives while reducing false negatives, and vice-versa. In general, a false positive is less of a concern than is a false negative, as failing to identify an explosive may lead to catastrophic results. However, the sensitivity and specificity of the system can be tailored to each situation. For instance, one would likely use a higher cut off value at a checkpoint in an area where the use of explosives is likely, such as a secured embassy or forward operating base. On the contrary, one would generally be willing to accept more risk and lower the cut off value at a screening point at a small rural airport.

CHAPTER 3 - Designing the Lab Prototype

Many parts must be brought together to develop a prototype explosive detection system using the SBRS approach. First, radiation sources are required to generate the signatures from unknown samples. An array of detectors is needed to measure the back-streaming radiation from the targets. Finally, a facility where the equipment can be safely operated is required. This facility must provided adequate space for the required equipment as well as shielding to protect the lab workers from exposure to harmful levels of radiation.

3.1 Goals of the SBD Project at Kansas State University□□

Simulations have shown that signature based radiation scanning (SBRS) can be used to distinguish explosive from inert materials in bulk sizes. (Johl 2009) The next step in the research is to construct a prototype device that uses the techniques proven in simulation to interrogate targets and determine whether the targets are safe or explosive. There are two primary concerns when designing the prototype. The first is that it should have a high sensitivity and specificity, with a higher priority toward sensitivity. In other words, while it is important to minimize false positive readings, it is even more important to ensure there are no false negative readings. The second concern is to achieve standoff of 1 meter or more. This means that no part of the prototype can be within 1 meter of the target to be interrogated. The size of the prototype is not a large concern, because it can be minimized after the technology is proven.□□

3.2 Overview of the Lab Prototype Design□□

The lab prototype is to be built in a three-room lab on the Kansas State University (KSU) campus. The first room will be the target room, with a translation stage and the unknown samples. The second is an equipment room containing the radiation sources and detector array. Finally, the third room is a control room from which operators can conduct experiments. There are four main components of the prototype: a machine gamma source, a machine neutron source, an array of detectors and a translation stage where targets can be scanned. The gamma ray source, neutron source and detector array are arranged in the equipment room so that the gamma source and neutron source are aimed at the target and the detector array is between them to minimize the angle between the forward and reflected radiation. The wall between the equipment

room and the target room acts as the plane of separation to achieve at least 1 meter of stand-off. The target room has a beam catcher and a translation stage for the targets. The translation stage can move targets horizontally with respect to the radiation sources to simulate scanning of larger targets, such as a vehicle. Behind the target is a beam catcher, which moderates the neutron beam in order to keep radiation levels outside of the room at safe levels. Figure 3.1 shows an overhead view of the equipment room and target area, as well as the position of the two sources and the detector array. Additional equipment racks will be placed in the room with the sources. These include power supplies, chillers for coolant lines to the neutron generator and control panels for opening and closing valves used during maintenance.

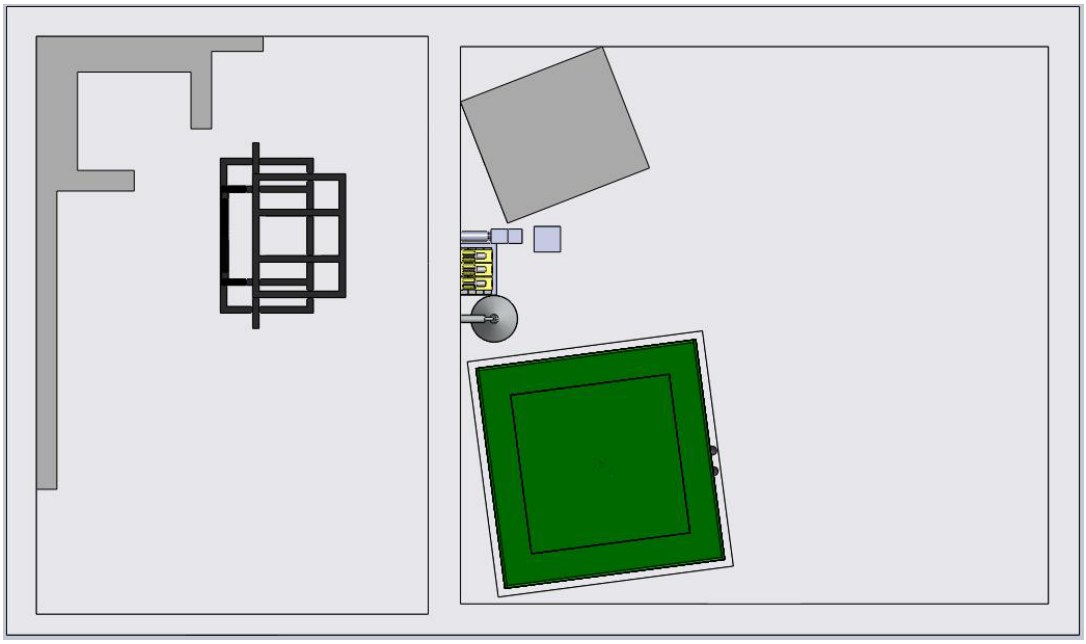

Figure 3.1 This overhead view shows the arrangement of the target area (left) and the equipment room (right). The neutron source (lower right) and gamma ray source (upper right) are collimated so that the beams intersect at the target stage.

3.2.1 Gamma Source

A 5-MV Betatron was originally chosen as the gamma source for the possibility of inducing PIPAR in the target. However, the results from the Betatron proved to be unrepeatable due to inconsistent gamma ray flux from the Betatron. Also, despite the high gamma-ray energy, PIPAR was not clearly observed in any of the experiments. Due to the Betatron not providing any useful results, a lower energy gamma source could be used, as long as it provided consistent gamma ray flux, within acceptable statistical variance. Both radioisotope and machine source

were considered to replace the Betatron. A few experiments were conducted using radioisotopes, but in the end a machine source was preferred. The source chosen was a 450 keV x-ray tube from GE.□□

3.2.2 Neutron Source□□

The neutron source chosen for the SBD lab is the Adelphi DT-111 machine neutron source. This source was chosen because of its high neutron flux and neutron energy. The function of the DT generator is explained more thoroughly in chapter 4. The high neutron flux increases the number of particles striking the target, which increases the probability of particles being emitted into the solid angle of the detector array. The high energy of the neutrons allows them to penetrate deep into targets and to excite high energy inelastic scatter gamma-rays.□□

3.2.3 Detector Array□□

The detector array consists of two High-Purity Germanium (HPGE) Detectors, six 3x3 Thallium activated Sodium Iodide (NaI(Tl)) detectors, and two neutron detectors, one bare and one cadmium covered. The HPGE detectors provide the high energy resolution needed to identify characteristic prompt capture and inelastic scatter gamma rays. The NaI detectors are more efficient than the HPGE detectors, so more gamma rays will interact with them. This allows faster acquisition of backscatter signatures. The neutron detectors are used to measure neutrons reflected from the target.□□

3.2.4 Target Area□□

The target area is in a separate room from the radiation sources and detectors. This is primarily a matter of convenience, but also demonstrates the ability to interrogate targets from a stand off. The unknown samples are placed on a mechanical translation stage that can move them in two directions. This allows scanning a larger target, such as a truck. Opposite the target from the neutron source, a beam catcher is built into the wall in order to capture any neutrons that pass through the target. This keeps the radiation levels outside the building within safety standards.□□

3.3 The Neutron Source Vault□□

Moderating and collimating 14.1 MeV neutrons requires a large amount of material. Monte Carlo N-Particle simulations were run to determine the appropriate amount of material for shielding the machine neutron source. A beam port is then cut into the shielding to collimate the isotropic neutron flux into a useable beam. Based on these simulations, a vault was designed to house the machine neutron source. This vault serves as both a moderator and collimator for the neutrons source.

3.3.1 Collimating 14.1 MeV neutrons

In order to produce a beam of 14.1 MeV neutrons, any neutrons emitted in a direction outside the intended beam must first be slowed down, and then absorbed. To shield the DT-111 Neutron Generator, a mixture of steel, high-density polyethylene (HDPE) and borated high-density polyethylene is used to slow and then absorb the neutrons, as well as absorb most of the gamma rays generated within the source and shielding. The ability of a material to slow neutrons can be characterized by its slowing down decrement, ξ. The slowing down decrement is the mean logarithm of the energy loss ratio, or ln*(E/E')*. The slowing down decrement can be estimated in terms of the mass of the scattering nucleus:

$$\xi = \ln\left(\frac{E}{E'}\right) \cong \frac{2}{A+\frac{2}{3}}, \tag{3.3.1}$$

where A is the mass number of the scattering nucleus. (Lewis 2008) This estimate is accurate to about 3% for A=2 and the error decreases as the mass number increases. It is clear that neutrons lose more energy when they scatter off of light nuclei rather than heavier nuclei. For this reason, HDPE is a good material for slowing neutrons because of the high concentration of elements with light nuclei, particularly hydrogen. Layers of heavy elements, such as iron, placed within a hydrogenous medium can remove fast neutrons (Shultis and Faw 2000). Iron also shields the gamma rays produced by inelastic scatter and neutron capture within the vault. Once the neutrons are slowed, they must be absorbed by a neutron absorber. Boron has a high cross section for capturing thermal neutrons. Borated HPDE is placed on the outside of the shield, so that after being slowed to thermal energy, the neutrons can be captured by boron in the HDPE.

3.3.2 Collimating Isotropic Emissions into a Beam

The neutrons created by fusion reactions are emitted essentially isotropically from the location of the fusion reaction. In order to create a useable beam, a small hole is cut through all layers of the shielding to allow neutrons to stream through towards the target. There are three different neutron-producing fusion reactions, discussed in the next chapter, as well as neutrons that will scatter off of the wall of the vault opposite the beam port and into the solid angle of the beam port. Although 14.1 MeV is the most probable neutron energy, based on the reaction cross-sections, this beam will have a spectrum of neutron energies.

3.3.3 Construction of the Vault

Layers of steel, HDPE and borated HDPE placed around the machine source moderate the 14.1 MeV neutrons and collimate them into a usable beam. Monte Carlo N-Particle (MCNP) simulations were used to verify that the thickness was adequate to reduce radiation outside the vault to safe levels (Johl 2009). The materials used to shield neutrons are alternating layers of HDPE and low carbon steel, as shown in Figure 3.2. Each layer is two inches in thickness. The very outside layers are borated HDPE to absorb the thermalized neutrons. This design is adequate to shield a 14.1 MeV isotropic point neutron source with a source strength of 10^{11} neutrons per second. However, this design must be modified slightly in order to house the machine itself as well as provide access for the power, cooling and control lines required to operate the DT-111. A circular hole must be cut out of the first five layers, or 10 inches, directly beneath the source cavity to make room for high voltage and cooling lines. A rectangular section must be removed from the subsequent 4 layers, or 8 inches, so that conduits can be running under the floor to the base of the vault for these power and cooling lines. This void beneath the detector can be filled with borated paraffin wax, to compensate for the removal of shielding material. In addition, a large portion of the shielding above the DT-111 must be cut away to make room for the microwave source that extends from the top of the DT-111, perpendicular to the axis of the cylinder. Lastly, the beam port itself must be cut from the shielding. In order to provide the best possible collimation, the beam port is cut parallel to the ground along the diagonal of the vault. This allows for the maximum collimation length.

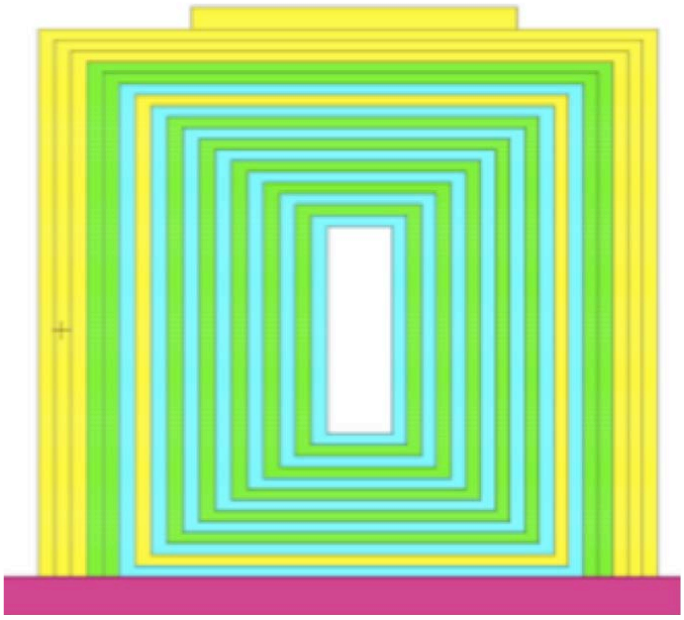

Figure 3.2 This side view shows the design of the shielding as created and tested using MCNP5. Each layer is two inches in thickness. The outermost three layers are borated HDPE, followed by two layers of HDPE, then a layer of steel, a layer of borated HDPE, and then alternating layers of steel and HDPE. The thick bar at the bottom is the concrete slab beneath the vault.

The construction of the vault is limited by availability of materials as well as production techniques. The MNCP simulations considered materials that were ordered slabs. HDPE is readily available in one-inch thick sheets. However, most manufacturers of radiation shielding provide borated HDPE at five percent boron by mass. Due to the high neutron flux and limited space available for shielding, sheets of HDPE borated to eight percent by mass were desired. Also, manufacturers typically produce HDPE sheets in one-inch thickness, as opposed to the two inches required by the MCNP simulation. This is easily overcome by placing two one-inch sheets next to each other to create the required two-inch thickness. Steel is readily available, and can be rolled into any thickness required, however, the largest sheet required to create a side of the designed vault is 88x88 inches. A sheet of steel two inches thick, and 88 inches in length and width would weigh well over 2000 pounds. Also, welding two inch thick steel sheets together is very time consuming and difficult. For ease of handling and assembly, steel sheets were ordered

that were 0.5 inches in thickness. Some handling equipment is still required, such as an overhead lift, but the heaviest sheet is around 800 pounds, which is a much more manageable weight.□□

While the floor can be modified to support the weight of the entire vault, each layer must be able to support its own weight. To accomplish this, a "stair-stepped" pattern was applied to each layer of the vault. As shown in Figure 3.3, the top and bottom of each layer are of sufficient length and width so that the sides rest on like material. This way, heavy steel is not resting in plastic, which may cause settling issues. For stability and to protect the neutron source, the innermost layer of steel is fully seam welded around all sides. However, because each layer of the vault is alternating steel and plastic, there is some concern that the heat from welding the steel together could melt the plastic and create streaming paths for neutrons. In order to limit this, the subsequent steel layers are stitch welded. Each two-inch steel layer in the MCNP simulation is actually constructed from four one-half inch steel sheets. The first, or inner most, sheet of each steel layer is only "tack" welded, to hold it in place while the other three sheets are put in place. Each of these three layers is "stitch" welded, to provide adequate strength while minimizing the amount of heat produced during welding. The outer most layers are borated polyethylene, which were cut to size by the manufacturer and are heat sealed to ensure that streaming paths are minimized.□□Further details on the construction of the vault are presented in **Error! Reference source not found.**.

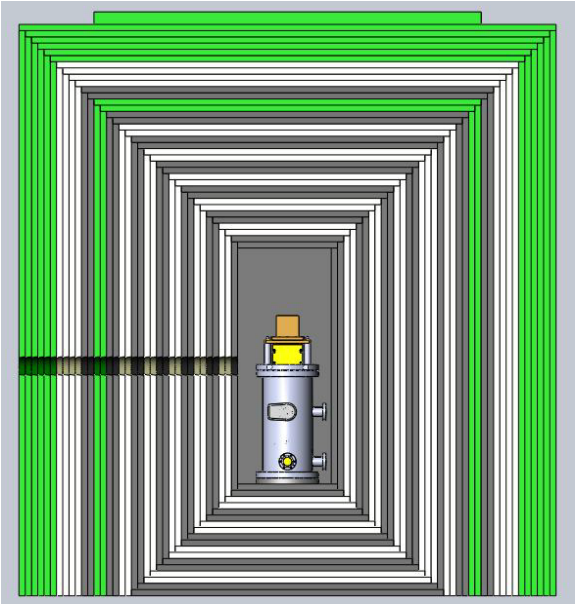

Figure 3.3 These side views show a more detailed technical drawing of the actual assembly of the vault using 1” thick sheets of steel and plastic. In actuality, each 1” layer of steel is comprised of two 0.5 inch sheets.

One final concern is the fitting of the DT-111 within the vault. The original design was completed using MCNP with the understanding that the DT-111 was generally cylindrical and would fit within the 16”x16”x38” interior cavity. However, the final design of the DT-111 includes several components that will not fit within this volume. The principle concern is the microwave source, which extends horizontally from the top of the neutron source for approximately two feet. In order to allow for the maximum shielding around this microwave generator with the least modification to the existing shielding, the DT-111 must be placed so that the microwave generator extends along the diagonal of the vault, opposite the proposed beam port. Also, small amounts of shielding must be cut away from the interior layers of steel to make room for an ion pump and SAES getter. The function of these components is explained further in Chapter 4. □□

3.4 Modifications to King Hall Annex

The laboratory prototype is being built in King Hall Annex on the KSU campus. This building was originally designed as a chemical storage building. It offers many advantages, such as large open rooms for equipment and heavy concrete walls that aid in shielding radiation.

However, many changes had to be made in order for King Hall Annex to house the laboratory prototype, including additional radiation shielding and reinforcing the floor to support the weight of the neutron source vault.□□

3.4.1 Flooring□□

The total weight of the steel and plastic needed to construct the neutron source vault is approximately 70000 pounds. Due to the large mass of the neutron source vault, it was determined that the flooring in King Hall Annex should be reinforced. To do this, a small area of the concrete floor was excavated. The base beneath the floor was compacted to provide better stability and a new concrete slab was poured in the excavated area. This provided several advantages. First, King Hall Annex was initially designed as a chemical storage building. To that end, the floor in room 107, where the vault is to be built, has a significant slope to it, for drainage purposes. The new lowered surface is flat, eliminating the concern that the mass of the steel may cause the layers to shift during construction or place additional stress on the welds. Second, the lower surface provided more clearance above the top layer of the vault for material handling equipment used when placing the heavy sheets of steel. Third, lowering the floor lowers the height of the neutron beam, reducing the shielding requirements on the roof of the building.□□

3.4.2 Shielding the Walls and Roof□□

Although the designed source vault moderates the neutrons coming from the DT-111, there still exists an unsafe level of radiation within the equipment room and target room. In order to ensure that the radiation levels outside the rooms remain safe, the roof and any doorways into these two rooms required additional shielding. In addition, a beam catcher is placed on the opposite side of the target from the neutron generator. As mentioned earlier, King Hall Annex was designed to store chemicals, so the roof of the equipment and target rooms feature blowout panels, designed to allow energy an easy path to escape the building in the event of an explosion. These blowout panels are made of thin plastic and provide little radiation shielding. In order to reduce sky shine, these voids were filled with polyethylene. Directly over the source, a mixture of virgin and borated HDPE is required, as the neutron flux is intense at there. The thickness of plastic required is reduced in the voids that are not directly over the source.□□The doors and HVAC openings in Room 107, the equipment room, must also be sealed. The HVAC ducts are sealed with HDPE, while the outer doors must be covered with concrete and HDPE. Sliding

shield doors are placed over the doors into the hallway to allow access to the equipment and target rooms as needed.

CHAPTER 4 - The Adelphi DT-111 Neutron Generator

Kansas State University has contracted Adelphi technologies to develope a one of a kind 14.1 MeV neutron source for use in SBD research. The DT-111 uses fusion reaction of hydrogen isotopes to create a high neutron flux, up to 10^{11} neutrons per second. By using a mixture of tritium and deuterium gas, the DT-111 generates neutrons with a range of energies, from 2 to 14 MeV.□□

4.1 General Operation of the DT-111□□

The DT-111 Generator uses the fusion of deuterium and tritium to create 14.1 MeV neutrons. In order to create the fusion reaction, the hydrogen atoms must be accelerated with enough kinetic energy to bring the two nuclei close enough together for tunneling to occur. To do this, the deuterium and tritium atoms are given a positive charge, and then accelerated through an electric potential field toward a target. The target is made of a hydride, in which the hydrogen isotopes become imbedded. As the isotopes continue to be ionized and accelerated towards the target, they will reach an atom density sufficient for subsequent ions to collide with them. The kinetic energy of the isotopes is sufficient to bring the two nuclei close enough together for tunneling to occur, enabling the fusion reaction. □□

There are several possible interactions on the target. The fusion of a deuterium and a tritium nucleus, or D-T fusion, results in an excited ^{5}He nucleus. The ^{5}He nucleus quickly decays to the ground state by emitting and 14.1 MeV neutron. The fusion of two deuterium nuclei, or D-D fusion, results in a ^{3}He nucleus and a 2.45 MeV neutron with 50 percent probability and a ^{3}T nucleus and a proton with 50 percent probability. Although the contribution is small, due to the small cross section for D-D fusion, the tritium produced in D-D fusion will re-circulate into the ionization chamber and contribute to subsequent D-T fusion. The fusion of two tritium nuclei, or T-T fusion, produces a ^{4}He nucleus and 2 neutrons. The total energy of the reaction products from T-T fusion is 11.4 MeV, however, it can be divided among the three particles in an infinite combination of energies. Thus the neutron energy from T-T fusion ranges from about 2 MeV to about 10 MeV. □□Based on the cross sections for the different interactions, D-T fusion is the most probable reaction. At 100 keV, the microscopic cross section for D-T fusion is 3.43 barns.

At the same energy, the cross section is 3.3 x 10^{-2} barns for the D+D→T+p reaction, and 3.7 x 10^{-2} barns for the D+D→^{3}He+n reaction. The cross section for T-T fusion is 3.4 x 10^{-2} barns at 100 keV (Atzeni 2004). So, the cross section for the desired D-T reaction is two orders of magnitude larger than that of the other 3 possible reactions. If the gas is an equal mix of deuterium and tritium, the D-T reaction will dominate. The relative probabilities of neutron energies in a D-T generator are shown in Figure 4.1.

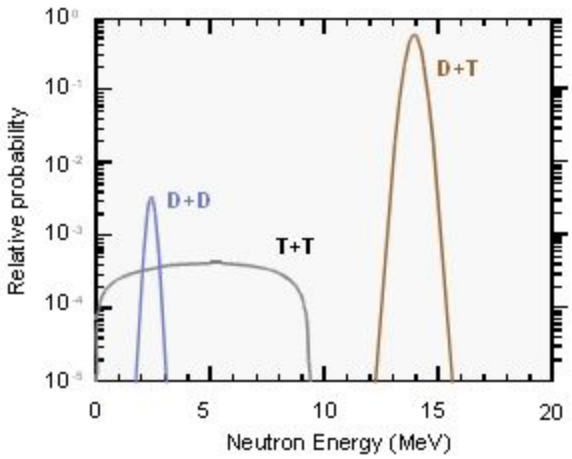

Figure 4.1 Provided by Adelphi Technologies, this figure shows the relative probability of neutron energies from a D-T generator.

In all three cases, helium is produced from the fusion reaction. This helium build up will degrade the performance of the neutron generator if it is not pumped off. An ion pump is used to pump the helium away when the generator is not in use. The ion pump ionizes gases within the vacuum and traps them within a strong magnetic field. For this reason, it must be closed off from the rest of the system during operation, or it will trap the hydrogen isotopes as well. Atoms trapped within an ion pump cannot be retrieved. Thus, the hydrogen isotopes must be captured before the ion pump is exposed to the vacuum. This is accomplished using an SAES Getter, which removes active gases from a vacuum by absorbing them into a special alloy. The function of the getter is explained more thoroughly in the next section. For now it is sufficient to state that hydrogen can be trapped in the getter, and retrieved later by heating the getter material. The getter will not remove noble gases, such as helium, as they do not react with the getter material. This allows the ion pump to remove the built up helium without removing the hydrogen isotopes from the system.

4.2 Functions of Specific Components of a Neutron Generator

In order to set the condition for the fusion of hydrogen isotopes to occur, several key components of the DT-111 must work in concert. The gas must be ionized, accelerated through a potential field and finally the atoms must be allowed to collide in order to create fusion. The fusion reactions discussed above cause the build up of helium gas, which must be removed in order to continue to operate the generator at peak efficiency.

4.2.1 Ionizing the Hydrogen in the Electron Cyclotron Resonance Ion Source

In order to be accelerated through a potential field, the hydrogen isotopes must be ionized. The Electron Cyclotron Resonance (ECR) Ion Source ionizes the gases by creating high-density plasma from the hydrogen isotopes. Microwaves are injected into a magnetic field within the plasma chamber. The microwaves enter the chamber through a dielectric window. This window must create a vacuum seal with the chamber as well as permit microwaves into the chamber. If the magnetic inductance is properly matched to the microwave frequency, the free electrons within the chamber will be accelerated in a circular motion within the chamber. The magnetic inductance required to meet the ECR condition is given by:

$$B_c = \frac{m\omega}{e}. \tag{4.2.1}$$

Here, B_c *is* the critical magnetic inductance, m and e are the electron mass and charge respectively and ω is the frequency of the microwave source. (Taylor 1991) These free electrons will continue to accelerate until they are energetic enough to ionize the gases by removing an electron. The electrons ejected from the hydrogen isotopes will also be accelerated in a circular motion, contributing to increased ionization. The ions can then be extracted from the plasma chamber via a potential field.

4.2.2 Extracting the Ions and Protecting the ECR Source

The ions are collimated into a beam via a small iris on the opposite end of the chamber from the dielectric window. The voltage potential at the iris is 0 kV and increases closer to the target. As the positively charged ion beam passes through the vacuum chamber, it will ionize some of the neutral gas between the target and the extraction iris, freeing electrons in the vacuum. A small fraction of the ions may also strike the outside of the metal shroud around the target, freeing secondary electrons. These electrons will back-stream through the extraction iris

and strike the microwave window, potentially damaging it. The microwave window is typically made of either quartz or alumina .A ceramic layer, typically made of boron-nitride, is placed on the plasma side of the dielectric window to protect it from the back-streaming electrons. Boron nitride has several properties that make is desirable as a shield. First, it is very easy to machine, and can be cut and shaped with metal working tools. Second, BN has a high resistance to heat. (Taylor 1991) A quartz dielectric window also has a high resistance to heat, but the BN shield is used so to protect the quartz window from back-streaming electrons so that the quartz will still maintain the vacuum seal, even if the BN is damaged. Both quartz and Boron-Nitride have a high probability of dissociating molecular H_2 when it strikes the surface, which increases the percentage of hydrogen atoms, which are more easily accelerated through the voltage field. The disadvantage of both quartz and boron-nitride is their poor heat conduction, which can cause them to overheat and crack if the intensity of the back-streaming electrons is too great. In this case, alumina may be preferred due to its high relatively high heat conduction.

The positively charged ions will strike the target with enough energy to free electrons from the metal surface. If not suppressed, these secondary electrons will stream back into the plasma chamber, increasing the intensity of the electrons striking the window 2 to 3 times. Back-streaming electrons can also cause sparking, and damage to the iris. While nothing can be done about the electrons caused by the ion beam, the secondary electrons can be suppressed to reduce these effects. A dome shaped metal shroud is placed around the target to suppress these secondary electrons. There is a small opening at the apex of the shroud to allow the ions to pass through. The shroud is charged to a slightly higher negative charge than the target, so it repulses the electrons coming of the target, preventing them from streaming back into the plasma chamber. The higher negative charge of the shroud will cause the ions to diverge slightly from the beam toward the target, but the energy of the ions is very large when compared to an electron. They have enough momentum to continue to the target rather than being pulled into the shroud. Figure 4.2 shows a cut away of the iris shroud and target, and the equipotential lines of the electric field. The potential is 0 V at the extraction iris, which is at the origin in the figure. The voltage potential of the target, on the right, is 117.6 kV while that of the shroud around it is 120 kV.

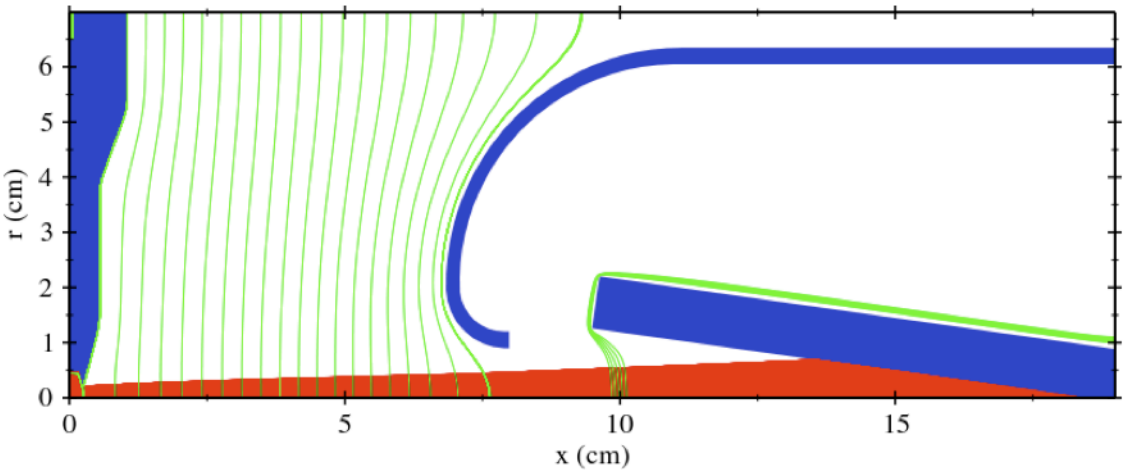

Figure 4.2 This simulation, created using IBSIMU, shows the equipotential lines within the DT-111.

4.2.3 Colliding the Ions on the Target□□

A negative voltage potential is applied to the target made of a metal hydride, such as titanium, so that the ions are attracted to it. A certain percentage of hydrogen ions impinging on the surface of the target will be captured in the lattice of the titanium. The penetration depth is typically less than 10 microns due to the relatively small potential field. The ions that are not trapped on the target will lose their positive charge due to coming in contact with the negatively charged surface. These now neutral hydrogen atoms or molecules will eventually recirculation into the Ion Chamber through diffusion. As the density of ions captured on the surface increases, the probability of a collision increases. The surface density of hydrogen on the titanium will eventually reach a saturation point at which the number of ions escaping the target is the same as the number impacting it via the ion beam. □□

Titanium is a poor conductor of heat; therefore it must be cooled in order to prevent overheating. The titanium is blasted onto a copper substrate, which can be liquid cooled to maintain acceptable temperatures on the surface of the target. If the target is not cooled, the ion beam can melt a hole in it, as shown in Figure 4.3.

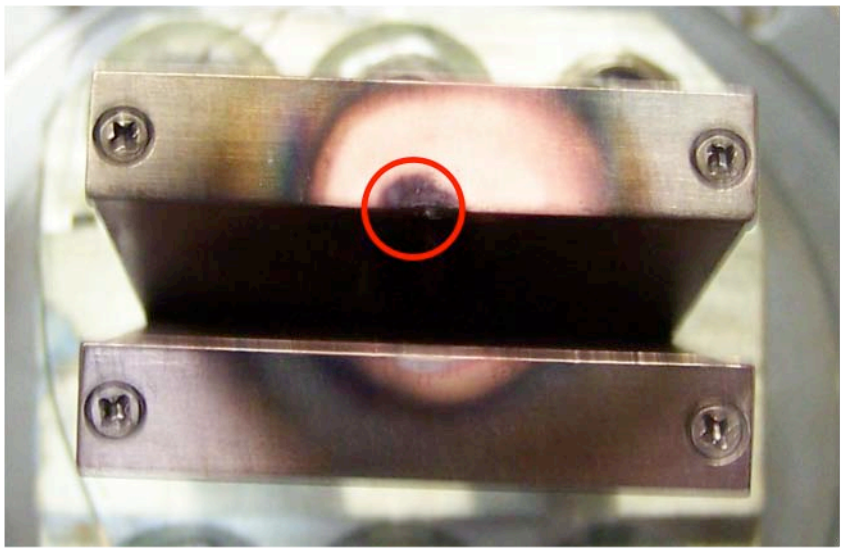

Figure 4.3 This target was left un-cooled during operation of a D-D fusion Neutron Generator. Note the burned away copper and titanium marked by the circle.

4.3 Gas Control Using an SAES Getter

One significant challenge for developing a Deuterium-Tritium neutron source is controlling the gas pressure within the chamber. In a deuterium only system, a regulator attached to a high-pressure gas bottle controls the pressure. The regulator is then connected to a stepper motor, and can be opened or closed to maintain the appropriate gas pressure within the system. The system is under active pumping, so if the pressure too high, the excess deuterium is vented into the lab. Tritium cannot be controlled using a gas bottle and regulator, because it is radioactive, and must be sealed within the system. In a single gas system, there is no need to monitor the mass fraction in the system because there is only one gas. When using deuterium and tritium, however, it is important to ensure that the mass fraction of each is roughly equal, to ensure the highest probability of a D-T collision. Thus, a new system of gas control must be devised that can control the pressure of Deuterium and Tritium without the use of external gas bottles.

4.3.1 Background on SAES Getters

Metal alloy getters are often used to augment mechanical pumps in vacuum systems to remove residual gasses after a mechanical pump down has reached its compression limit. These

alloys form chemical bonds with the active gases such as N_2, O_2, CO_2, and CO. These gases are permanently bonded to the alloy and cannot be released. Hydrogen and its isotopes do not form chemical bonds with the getter alloy. Rather, the getter pumps hydrogen out of a volume by storing it in a solid solution in the bulk of the material. The hydrogen can be released from the getter by increasing the temperature of the getter alloy. This reversible absorption of hydrogen into the getter material offers a possible solution for controlling the pressure of hydrogen isotopes within a sealed vacuum, eliminating the need for a pressurized gas bottle.

4.3.2 Methodology for Gas Control

When heat is applied to the getter, the speed at which it pumps hydrogen out of the system increases; however, the amount of hydrogen that can be stored within the getter material is reduced. Thus, the hydrogen is not released by heating the getter; rather it reaches an equilibrium pressure where the getter is out-gassing at the same rate that it is absorbing the hydrogen. This equilibrium pressure varies based on the temperature of the getter and the amount of hydrogen within the getter alloy. Sievert's Law describes this relationship (SAES):

$$Log(P) = A + 2Log(q) - \frac{B}{T}. \tag{4.3.1}$$

Here P is the equilibrium pressure of hydrogen in Torr, q is the concentration of hydrogen in the getter alloy in torr-liter per gram of alloy, and T is the temperature of the getter alloy in Kelvin. A and B are constants determined by the make up of the getter alloy. Figure 4.4 shows the relationship between hydrogen concentration within the getter material and equilibrium pressure for some common operating temperatures. Note the embitterment limit on the right side of the graph. When the hydrogen concentration within the getter reaches this limit, it will alter the physical properties of the alloy, causing it to become brittle and flake off from the metal substrate.

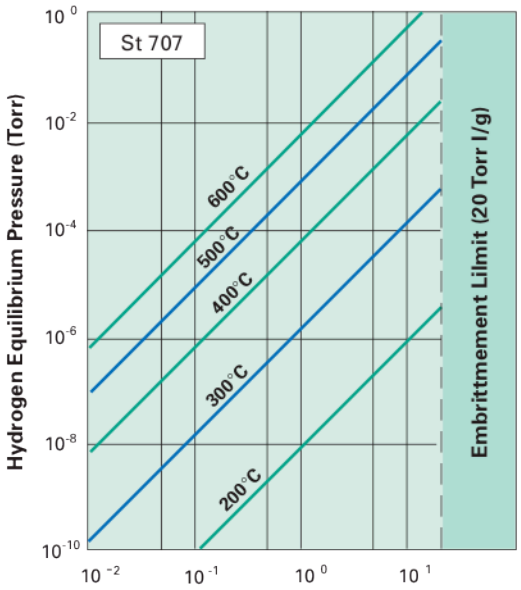

Figure 4.4 The equilibrium pressure of hydrogen increases with the concentration of hydrogen absorbed in the getter.

From this relationship, it can be seen that by varying the temperature of the getter, the equilibrium hydrogen pressure can be controlled. For D-T fusion applications, the concentration of hydrogen in the getter material will slowly decrease over the life of the DT Generator, as deuterium and tritium are consumed by fusion reactions. To compensate for this, the temperature of the getter will need to be steadily increased as the concentration of hydrogen decreases in order to maintain the same equilibrium pressure. The change in concentration will be slow because the amount of hydrogen consumed in fusion is small compared to the amount stored in the bulk of the getter. □□

The challenge with using a getter is ensuring that the mix of tritium and deuterium in the system is equal, which maximizes probability of a D-T collision. If either deuterium or tritium dominates the mixture, the neutron flux as well as the neutron energy spectrum will be less than ideal. As discussed in the previous section, there are four possible fusion reactions in the DT-111. D-T fusion, which results in a helium nucleus and a 14.1 MeV neutron, D-D fusion, which can result in either a helium nucleus and a 2.45 MeV neutron, or a tritium nucleus and a proton, and finally, T-T fusion, which results in a helium nucleus and 2 neutrons, with total energy being 11.3 MeV. The D-T reaction produces the most energetic neutrons. Fortunately this reaction also has the highest cross section. However, if D_2 or T_2 dominate the gas mixture, D-D or T-T fusion

may dominate and cause a shift in the neutron energy spectrum. This will also lower the overall neutron flux because of the lower cross sections for the D-D and T-T reactions, reducing the number of fusion events.

4.3.3 Specific Application for the DT-111 Neutron Generator

The getter chosen for the Adelphi DT-111 Neutron Source was an SAES GP-50. This model is a cartridge holding 32 grams of a Zr-V-Fe alloy, which has an industry name ST-707. The cartridge includes a heating element which, when connected to a high voltage power supply, controls the temperature of the getter alloy. The temperature control is important, because the equilibrium pressure of hydrogen varies with temperature. Figure 4.4 shows the relationship between the equilibrium pressure of hydrogen and the temperature of the getter material. The minimum pressure to create plasma within the ECR source is approximately 3 mTorr. From the figure, the getter must be heated to at least 400 °C in order to achieve this minimum pressure. The higher the temperature, the lower the concentration of deuterium and tritium within the getter needs to be. However, in order to extend the life of the getter, it is preferable to operate at lower temperatures of around 450 °C. The required hydrogen concentration to operate at this temperature can be found by solving Equation 4.3.1 for q, *i.e.,*

$$q = 10^{\left(Log(P) - A + \frac{B}{T}\right)}. \tag{4.3.2}$$

Substituting T = 723 K, P = 3 mTorr, A = 4.8 and B = 6116, a hydrogen concentration of 3.5 torr-liters/g should yield the desired pressure. For an equal mixture of tritium and deuterium, the concentration of each should be half of the value of q for a given temperature. Figure 4.5 shows the theoretical relationship between q and T for the ST-707 alloy.

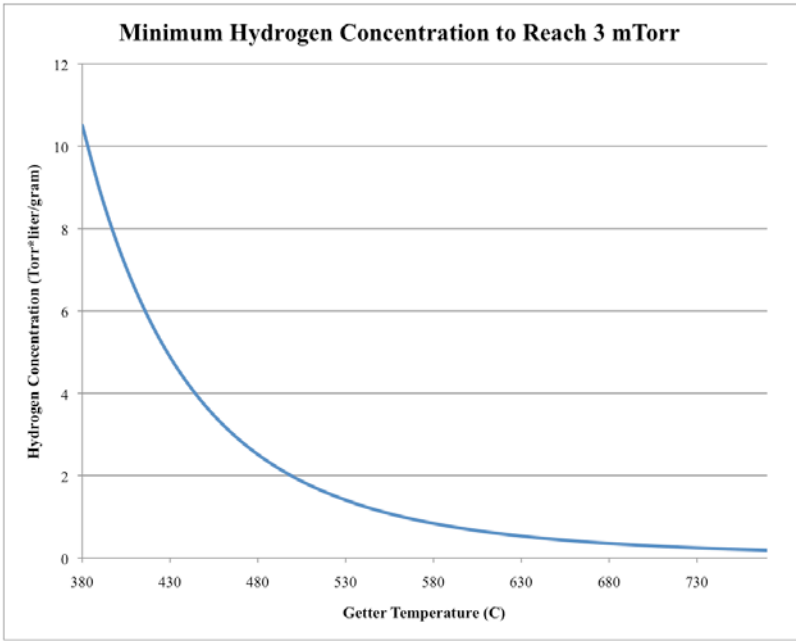

Figure 4.5 The required concentration of hydrogen decreases as the operating temperature of the getter increases.

4.3.4 Limitation of the GP50 for handling small volumes of Hydrogen

The amount of gas available for use in the DT-111 is limited by the tritium license held by Kansas State University. KSU can have a maximum of 10 Ci of tritium on hand at any one time. This presents a problem when using the SAES getter. The GP50 getter cartridge from SAES contains 32 grams of getter alloy. So, in order to reach the required concentration of 3.5 torr-liter/g, a total of 112 torr-liters of gas must be added to the system. However, 10 Ci of tritium is only 3.18 torr-liters. Adding the same amount of deuterium only brings the total to 6.36 torr-liters. Thus, the GP50 getter cartridge is too large for the given application. A custom getter, using around 1 gram of ST-707 would be more appropriate for the KSU DT-111 Neutron Generator.

4.3.5 Testing the Repeatability of Pressure Control using an SAES Getter

Although the GP50 is not suitable for use as a hydrogen source for the DT-111 Generator, it is still useful to experiment with it to further understand the behavior of the ST-707 getter when used as a hydrogen pump. The first thing to determine is whether or not the pressure inside the system can be controlled to sufficient precision. In order to determine this, a series of

experiments was conducted in which heat was applied to the getter, and the getter was allowed to out-gas until the pressure within the system equalized. □□

4.3.5.1 Experimental Procedure□□

The apparatus was assembled as shown in Figure 4.6. A valve is placed between the getter and the vacuum chamber so that, when the valve is closed, the hydrogen pressure in the system can be measured. Then, when the valve is open, the getter can to absorb the hydrogen. There is a pressure reducer in between the main vacuum chamber and the Residual Gas Analyzer (RGA) in order to keep the pressure on the RGA below 10^{-4} Torr. Above this pressure, the RGA can no longer measure individual mass peaks. Thus, while the actual pressure of hydrogen in the system cannot be measured, the atmosphere can be sampled so that the fraction of hydrogen can be determined. The system was assembled, heated and then allowed to pump down for 48 hours to ensure a clean vacuum.

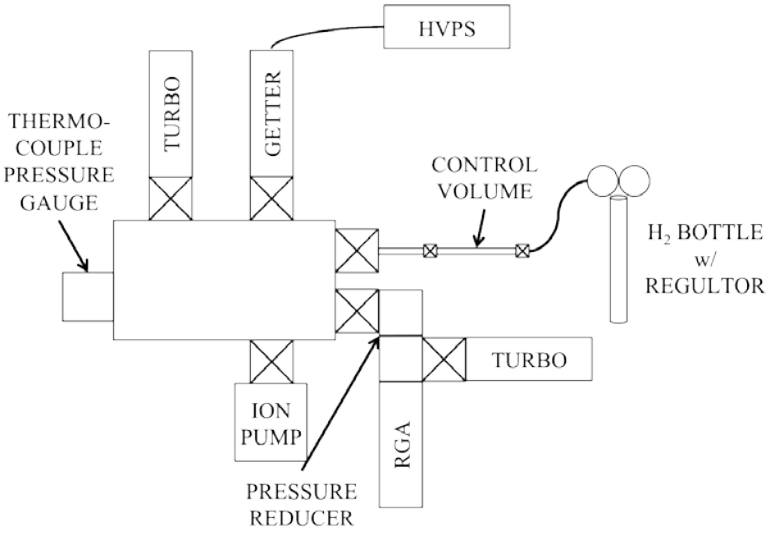

Figure 4.6 The experimental apparatus for testing H_2 pressure control using the GP-50 Getter.

For these initial experiments, hydrogen was used rather than deuterium because is more readily available and less expensive. Before any hydrogen was added to the system, the atmosphere was sampled and analyzed using the RGA. This provided a baseline for later comparison. Figure 4.7 shows the mass spectrum of the atmosphere before hydrogen was added. The horizontal axis shows the mass number, for instance 2 for molecular hydrogen. The vertical axis shows the partial pressure of particles at each mass number.

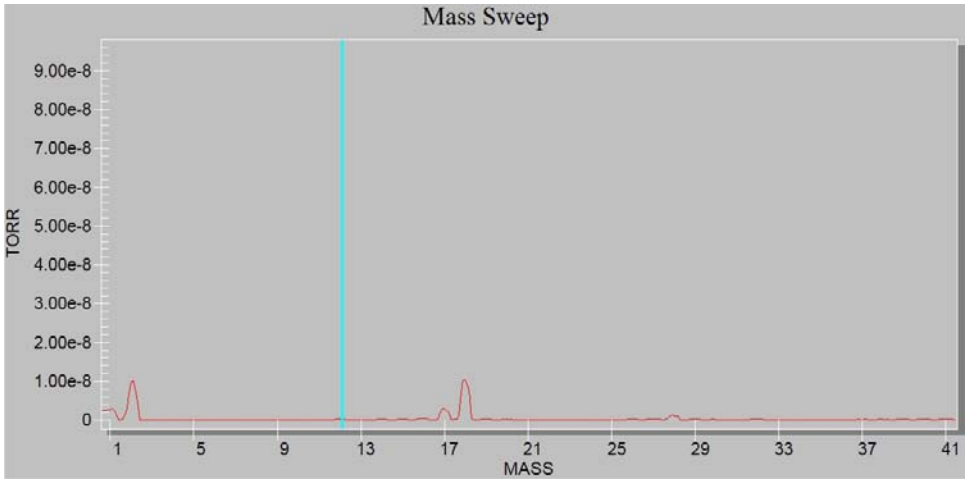

Figure 4.7 This mass spectrum shows the baseline atmosphere within the chamber before adding hydrogen. The only feature of note is the water grouping at masses 16,17 and 18.

To begin the experiment, a known quantity of hydrogen was added to the system. The goal was to add 1 torr-liter/gram of H_2 to the getter, or 32 torr-liters. The control volume is 3.18 ml. Thus, the required pressure within the control volume is:

$$\frac{32 \text{ Torr L}}{3.18 \times 10^{-3} \text{ L}} = 10063 \text{ Torr} = 194 \text{ psi}.$$

This is too large a pressure to measure on the regulator, so the hydrogen must be added in smaller amounts in order to be properly measured. In order to add measurable amounts of hydrogen to the system, 4 torr-liters were added at a time. So, the control volume was pressurized to:

$$\frac{4 \text{ Torr L}}{3.18 \times 10^{-3} \text{ L}} = 1257 \text{ Torr} = 24 \text{ psi}.$$

The pressure gauge on the regulator reads pressure above atmosphere, so in order to reach 24 psi, the pressure was increased until the gauge read 24 psi – 14 psi = 10 psi. The volume of the main vacuum chamber is approximately 13.4 liters, so if 4 torr-liters are added to this volume, the pressure within the chamber should reach 280 mTorr. When the first dose of hydrogen was added to the system, the pressure gauge read 593 mTorr. However, the thermocouple pressure gauge used to monitor the main vacuum chamber is calibrated for air, so the reading must be corrected for a pure hydrogen atmosphere. The manufacturer provided a nomogram, shown in Figure 4.8 (Teledyne Hastings 1974), for converting the pressure reading to the actual pressure. The actual pressure was approximately 300 mTorr, which is reasonably close to what was expected. The estimate of the control volume was likely lower than the actual

volume because it did not include the air space within the valves. This would account for the slight increase in the observed pressure. □□

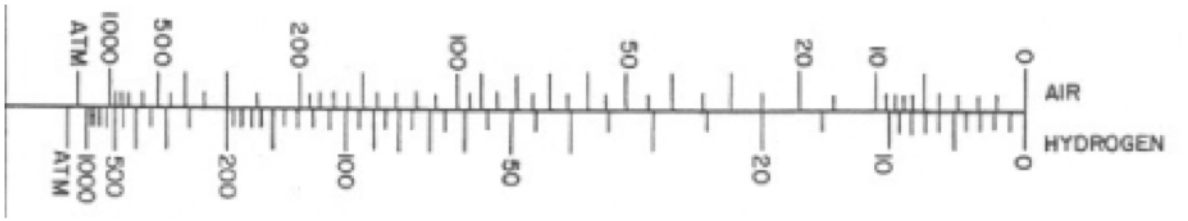

Figure 4.8 This nomogram, provided by Hastings Instruments, converts the reading on a gauge calibrated for air into the actual pressure in a hydrogen atmosphere.

Once the pressure was measured, the valve to the RGA was opened briefly to collect a sample of the new atmosphere within the chamber and then closed again to avoid pumping off the hydrogen that had been added to the system. The mass spectrum in Figure 4.9, showed an increase in the partial pressure of mass 2, or hydrogen, and was the same everywhere else, confirming that only H_2 was being added to the system through the gas inlet. The valve between the getter and the chamber was opened to allow the getter to absorb the hydrogen. Once the pressure in the main chamber was below 1 mTorr, the valve was closed and the procedure repeated for seven additional doses of H_2. When adding the third dose of H_2, the pressure in the chamber did not reach the expected 300 mTorr. The pressure rose immediately and then quickly fell to below 1 mTorr. The presumed cause of this was a leak in the valve between the getter and the main chamber, causing the getter to absorb the hydrogen as it was let into the system. However, the decision was made to continue with the test. As long as the control volume was pressurized to 10 psi gauge each time, it was reasonable to assume that the correct amount of H_2 was being added without having to check the pressure within the chamber. After the last dose of hydrogen was added, the system was left to pump down until the pressure was below 1 mTorr. □□

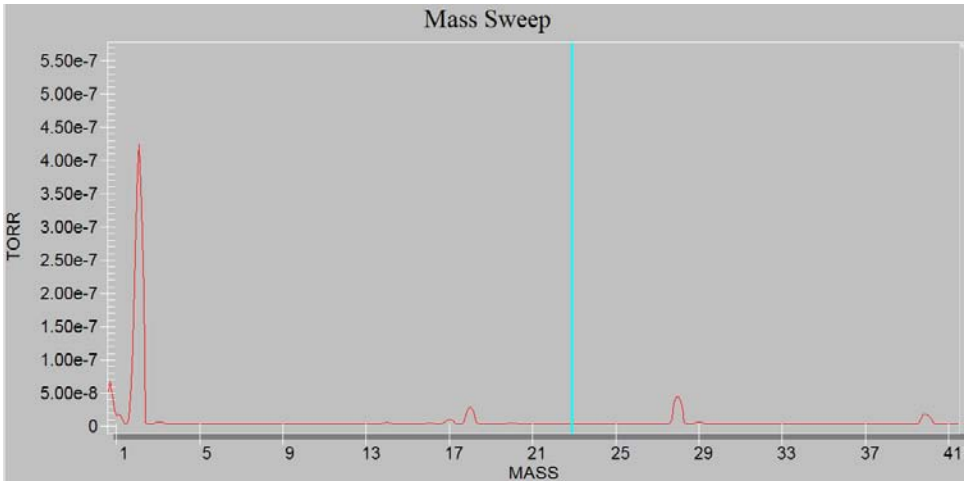

Figure 4.9 The mass sweep after the first hydrogen dose was added to the system. The only change from the baseline was the increase in the peak at mass 2, which corresponds to molecular hydrogen.

Once the hydrogen was absorbed within the getter, it was heated to a specific temperature and the pressure was monitored until it leveled off at some equilibrium. The getter is heated using an electric resistance heater. The relationship between temperature and voltage is provided by the manufacturer, and is shown in Figure 4.10. The correct voltage was applied to heat the getter to 500 °C, 550 °C, and 600 °C. Each temperature was repeated 5 times, and the equilibrium pressure recorded. Figure 4.11 shows the timed pressure curves for each temperature. □□

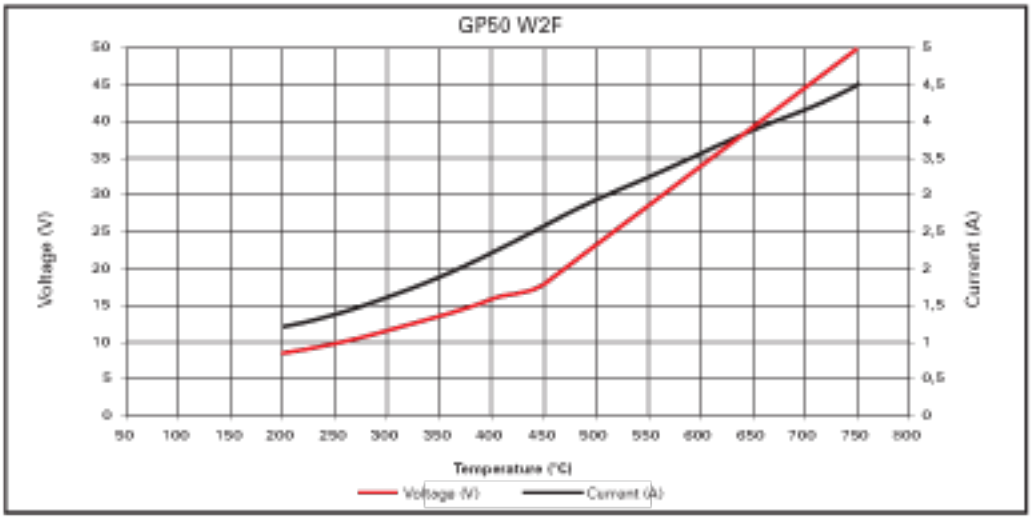

Figure 4.10 Provided by SAES, this curve shows the temperature of the heating element as it varies with voltage (lower curve) and current (upper line).

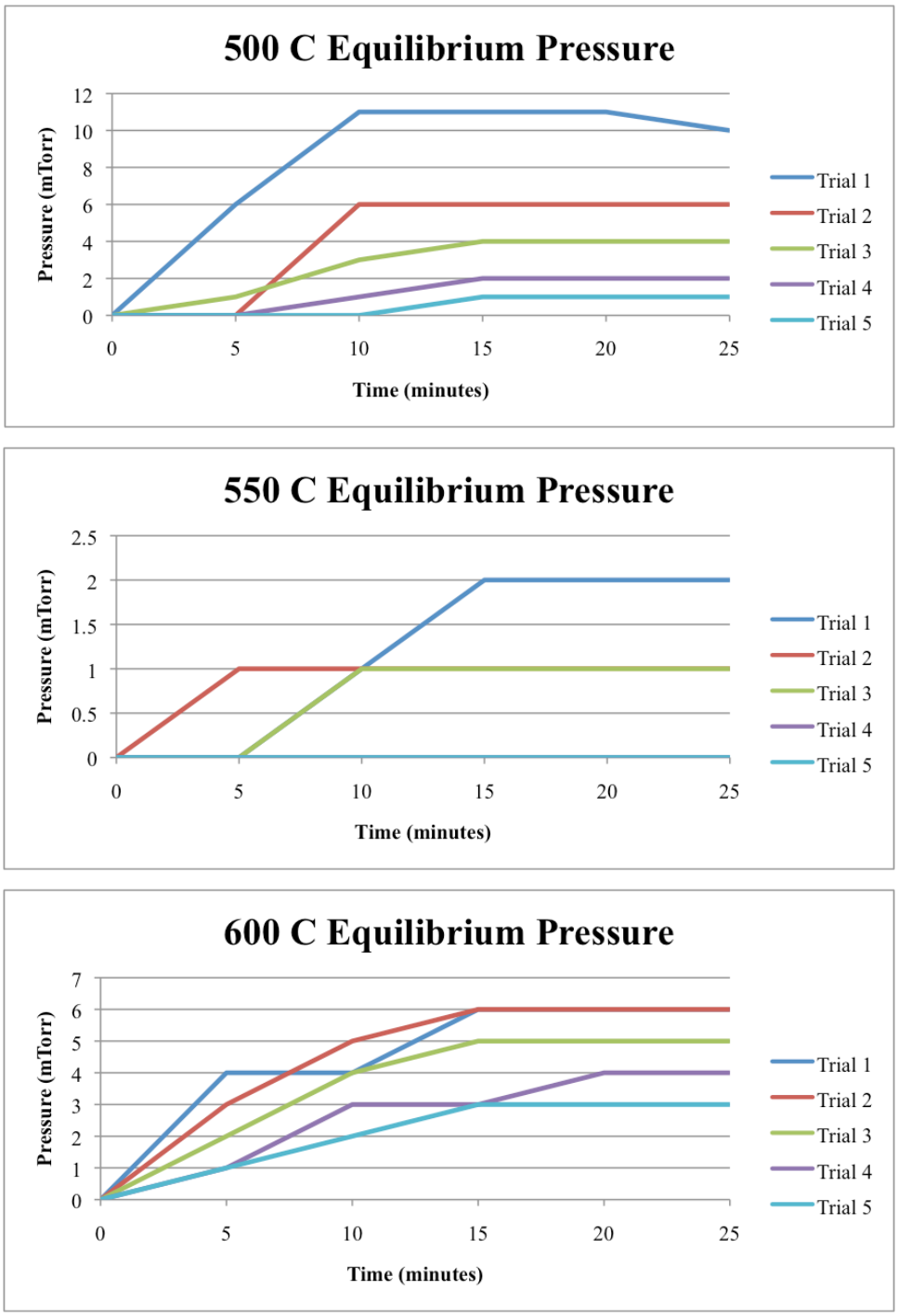

Figure 4.11 The pressure in the system increases slowly until it reaches equilibrium. However, note that the equilibrium pressure was lower for each subsequent trial.

4.3.5.2 Results of the Experiment and Lessons Learned

At each temperature, the equilibrium pressure decreased with each subsequent trial. There are two possible explanations for this. The first is that hydrogen is being lost from the

system during the out-gassing cycle. This is not likely as the pressure of the system is lower than atmosphere, so if there were a leak in the system, the mass sweep would have peaks corresponding to air, which were not observed. The more likely cause relates to a previous experiment in which a large quantity of hydrogen was added to the system. It is likely that during this experiment, the hydrogen concentration within the getter reached the 20 Torr-liters/gram embrittlement limit shown in Figure 4.4. When this limit is reached, the hydrogen absorbed within the getter changes the mechanical properties of the alloy (SAES). This causes the ST-707 to flake off from the stainless steel substrate. Separate from the substrate, the ST-707 will still absorb and expel hydrogen depending upon temperature. However, these flakes of ST-707 settle in the bottom of the stainless steel housing, and thus heat slower and cool faster than the getter material that is still attached to the substrate. The slower heating and faster cooling means that the equilibrium pressure of the flakes will be lower than the rest of the getter during heating and cooling, and thus these flakes will absorb hydrogen faster, taking it away from the remainder of the getter. This would cause the equilibrium pressure to be lower with each successive cycle of the getter, because the hydrogen concentration in the getter is reduced. This also explains why the valve between the getter and the chamber would no longer seal. It is likely that some flakes of ST-707 fell into the valve and obstructed the metal seal. □□

4.3.6 Correcting the Problem□□

A custom getter pump was designed to replace the GP50. Using a new getter with a smaller mass of ST-707, and ensuring that it was not loaded with hydrogen to the point of embrittlement, should correct the downward trend of the equilibrium pressure as well as allow the getter to reach equilibrium pressure in the millitorr range at temperatures much lower than would be required using the 32 gram GP50 cartridge. SAES offers ST-707 evaporated onto a stainless steel substrate in strips that are approximately 3 cm wide. These strips have, on average, 20 grams of ST-707 per meter. As previously stated, the maximum amount of gas available is 6.36 torr-liters. From Figure 4.5, the required concentration to reach an equilibrium pressure of 3 mTorr at 400 °C is approximately 7 Torr-liters/gram. Dividing the available gas volume by the desired concentration indicates that 0.9 grams of ST-707 will be adequate for the DT-111. A new getter, using the heating element from the GP50 and a sufficient length of getter strip to hold 1 gram of ST-707, should make it possible to control the hydrogen pressure within the DT-111.

The slight overdesign will ensure that the getter can hold all of the gas. If needed, operating the getter at a slightly higher temperature will increase the pressure. □

The redesigned getter, shown in Figure 4.12 uses many common components from the original GP50. The two primary advantages of using the existing platform are the ease and speed of manufacture and the well-established temperature vs. voltage relationship, shown in Figure 4.10. This new getter can be controlled using the same set up as the GP50, and housed within the same casing. Thus, it can be added to the system with minimal changes to the existing apparatus. □□

Figure 4.12 The original GP50 (a) with 32 grams of ST-707 shown next to the redesigned getter (b). The redesign uses 6 pieces of ST-707 for a total mass of approximately 1 gram.

4.3.7 Experimenting with the Re-Designed Getter□□

To begin, the new getter was assembled by cutting approximately 52 mm of the ST-707 strip, which will hold approximately 1.04 grams of ST-707, into 6 sections roughly 8.5 mm in length each. The apparatus is the same as the one shown in Figure 4.6, with two changes. First, the GP50 was replaced with the redesigned getter, and second, a cold-cathode gauge was installed on the same flange as the thermo-couple gauge. The cold-cathode gauge will read the vacuum below 1 mTorr, which is the lowest the thermo-couple will read. This allows for more

accurate monitoring of the gas pressure during the heating and cooling of the getter. Once assembled, the chamber was heated with resistive heating tapes and pumped down overnight. Prior to beginning the experiment, the atmosphere within the chamber was sampled as before to collect a baseline for later comparison. This background is shown in Figure 4.13.□□

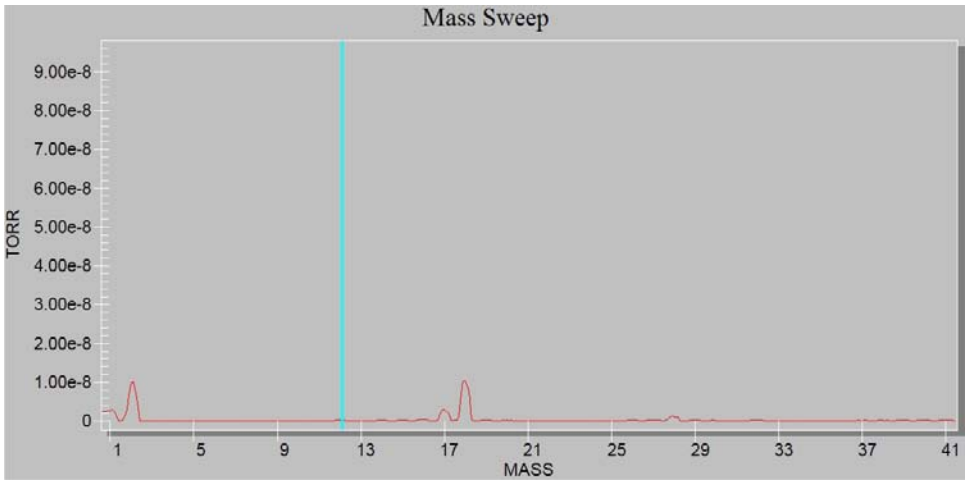

Figure 4.13 The baseline vacuum before adding hydrogen.

4.3.7.1 Setting Up the Experiment□□

The stated capacity of ST-707, according to the manufacturer, is 10 torr-liters/gram of alloy. In order to accurately simulate the gas volume available for the DT-111, approximately seven torr-liters were added to the system. To reach this, the control volume of 3.18 milliliters needs to be pressurized to 2160 torr, or 42 psi. Again, the regulator reads psi above atmosphere, so the pressure should be increased until the gauge reads 28 psi. However, similar to the previous experiment, the maximum pressure of the regulator is 25 psi. Thus the hydrogen was added in two doses. Each dose was 21 psi, or 7 psi on the gauge. When each dose of hydrogen was added, the pressure of the chamber again reached approximately 300 torr. The valve between the DT-111 and the RGA was opened to sample the atmosphere, shown in Figure 4.14 to ensure the only increase was at mass 2. Once the atmosphere was sampled, the valve to the RGA was again closed, and the valve to the getter was opened to allow the ST-707 to absorb the hydrogen overnight.□□

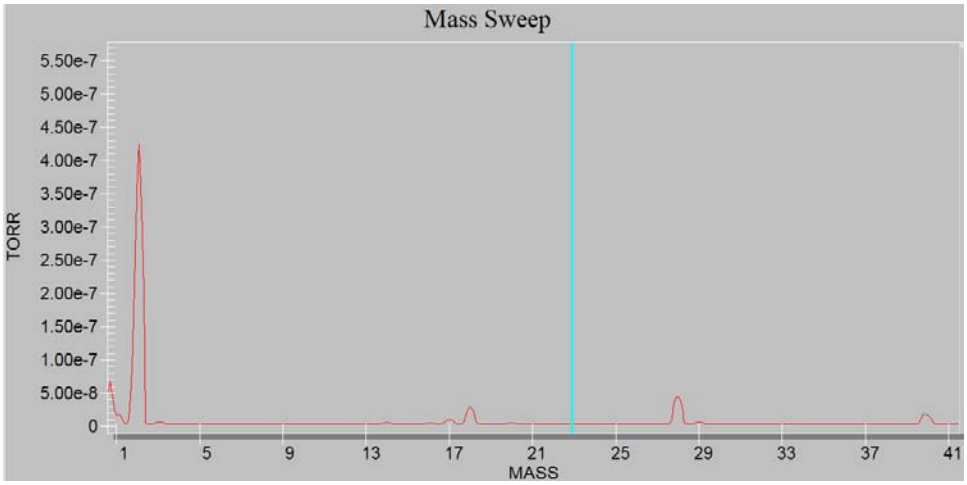

Figure 4.14 This mass sweep shows that only hydrogen is being added to the system.

For this experiment, the getter was only heated to 400 °C, which corresponds to applying 16 V to the heating element. The getter was heated and the pressure in the system recorded once per minute for 60 minutes, and then the getter was allowed to cool until the vacuum was below 10^{-5} torr. Once the pressure was below the cut off, the getter was heated again. During heating, the valve to the RGA was opened briefly to ensure that the increase in pressure was due to hydrogen. The mass sweep, shown in Figure 4.15, showed a peak at mass 2. This follows, as the only gases that are recoverable from the getter are hydrogen and hydrogen isotopes.□□

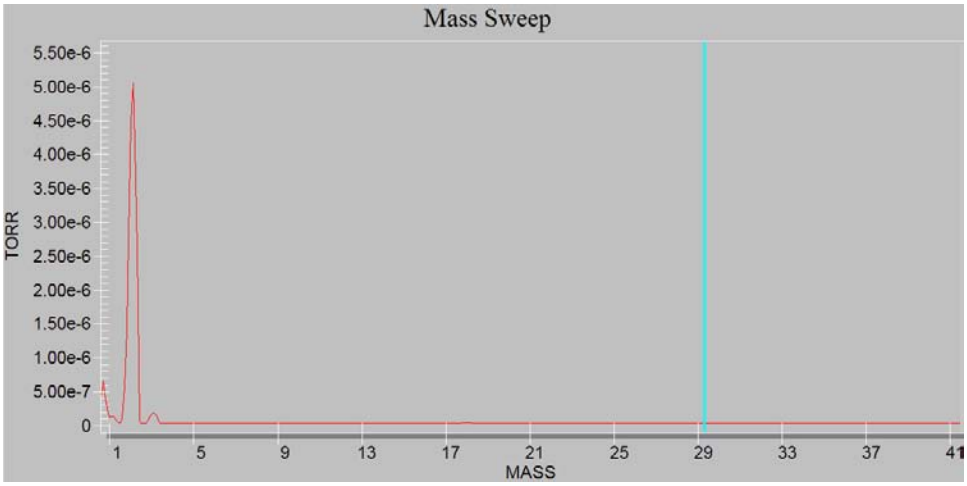

Figure 4.15 This mass sweep, taken as the getter was being heated, shows that hydrogen is being desorbed from the getter.

4.3.7.2 Results of the Experiment and Lessons Learned□□

The pressure vs. time plot for the five trials, shown in Figure 4.16 indicates that it is quite possible to achieve repeatable equilibrium pressure with a properly functioning getter. In the first

trial, denoted by the open circles, the getter had been cool over night, which explains the initially slow increase in pressure. In the subsequent four trials, the getter never reached room temperature, so the pressure increases more rapidly in these four trials. The curves also show the reduction in pressure for the first ten minutes after the voltage was removed from the heating element. It is clear that the pressure drops far faster than it rises. This is because the time constant for absorption is faster than that of desorption. It would seam that the disassociative absorption on the surface of the getter is the limiting factor in absorption. This allows the getter to absorb a great deal of hydrogen quickly. The plot shows that the pressure falls rapidly at first, and then the rate slows. This is due to the surface capacity being reached. As the hydrogen is diffused into solution in the bulk of the getter, more hydrogen can be absorbed on the surface. During desorption, the rate-limiting step is the speed at which hydrogen reaches the surface of the getter from the bulk, thus the slow increase during heating (Liu et al 2004).□□

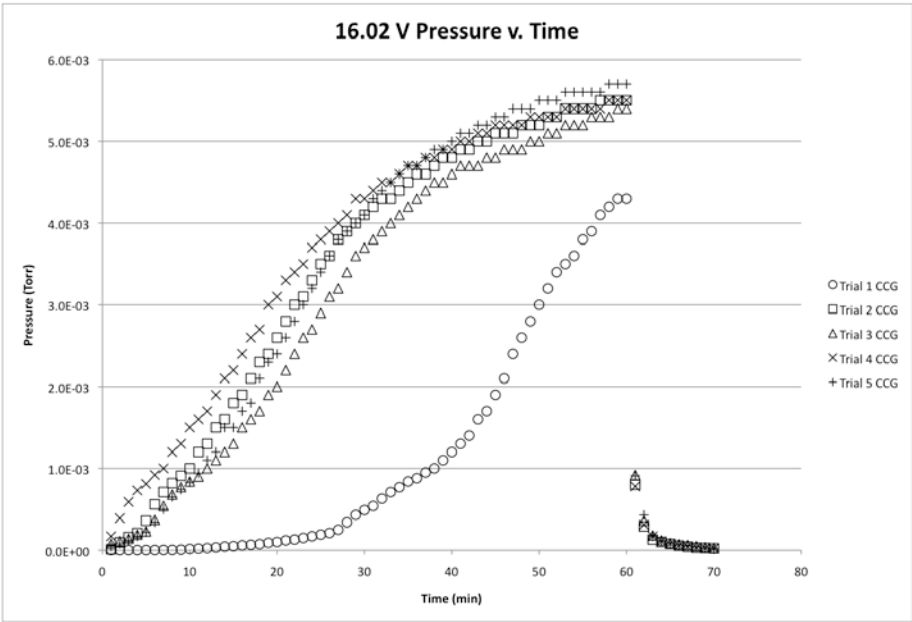

Figure 4.16 The gas pressure within the vacuum increases slowly when heat is applied to the getter and asymptotically approaches equilibrium.

Once repeatability was proven, the next step was to determine if the pressure can be controlled more precisely. This is a simple experiment using the same set-up as before. The getter is heated to 400 °C, and the pressure is allowed to rise to 5 mTorr or above. Once 5 mTorr is reached, the voltage is reduced to slow the rate of desorption. It is then a matter of monitoring the pressure. If it begins to fall below 5 mTorr, the voltage must be increased in small increments until it reaches 5 mTorr. The same is true if the pressure rises above 5 mTorr. The smallest

change in voltage allowed by the high voltage power supply is 0.1 V. The voltage was adjusted slowly until equilibrium was reached. For this getter, with the given concentration of hydrogen, an equilibrium pressure of 5 mTorr was maintainable at approximately 15.6 V. This is ideal because the operating pressure for the ECR source ranges from 3 to 10 mTorr.□□

Given the slow time constant for increasing pressure during heating, it is more practical to heat the getter once during a day of operating the DT-111, and keep it at temperature. If it is required for operators to go into the room with the neutron source, removing the high-voltage from the target will stop the neutron flux. Due to the long hold time, it is best to operate at relatively low temperature. There is a mechanical limit to how many times a getter can be cycled from cold to hot before the ST-707 begins to peel off from the substrate. This limit is reduced if the getter is operated at higher temperatures, or for longer periods of time. Figure 4.17 from SAES, shows how many times the getter can be cycled before peel-off begins, based on temperature and hold-time. Based on this chart, the getter can be operated almost indefinitely at 400 °C.□□

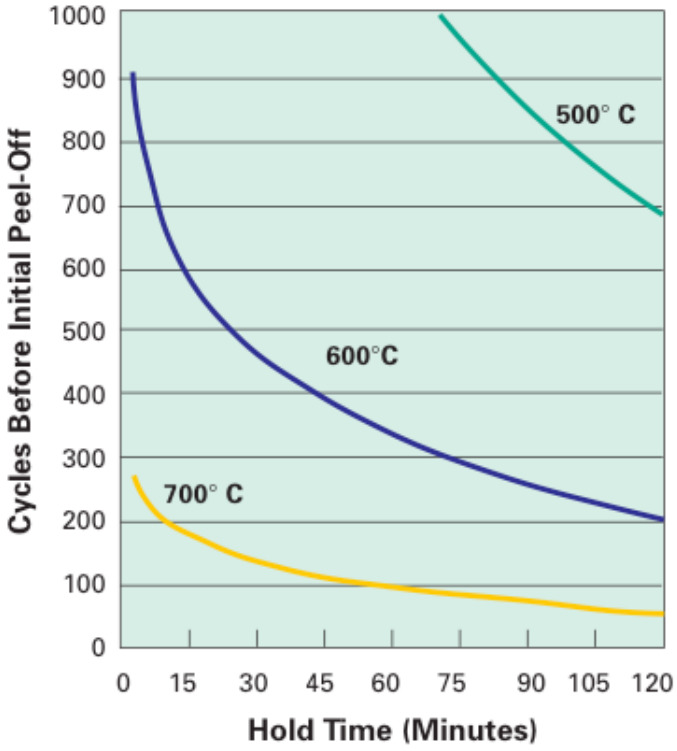

Figure 4.17 This chart, provided by SAES, shows the number of cycles before the ST-707 will be begin to peel off from the substrate. Operating at higher temperatures, or for longer times reduces the life of the getter.

4.3.8 Controlling Two Hydrogen Isotopes with the Getter

There is no physical reason for the getter to absorb different isotopes of hydrogen at different rates. Thus, it is reasonable to assume that loading equal volumes of tritium and deuterium will result in the proper gas mixture (Ferrario 1984). However, in order to ensure an equal mix of two hydrogen isotopes can be maintained, this assumption must be tested. Because the initial tests were conducted on an open system, hydrogen was used rather than tritium.

4.3.8.1 Experimental Procedure

The same apparatus used in the single-gas experiments was used in the two-gas test. The only change is the hydrogen bottle is removed after hydrogen is added to the system and replaced with a deuterium bottle. The getter used in the single-gas experiment was removed and examined to ensure there were no signs of embrittlement, which there were not. A new getter was constructed, this time using only 48 mm of ST-707, cut into six strips that were each 8 x 30 mm. Due to the smaller getter, only six torr-liters of gas were added to the system for this experiment, three of hydrogen and three of deuterium. With the getter closed-off from the system, 3 torr-liters of hydrogen were added, followed by 3 torr-liters of deuterium. The valve to the RGA was opened to collect a sample of the atmosphere, shown in Figure 4.18.

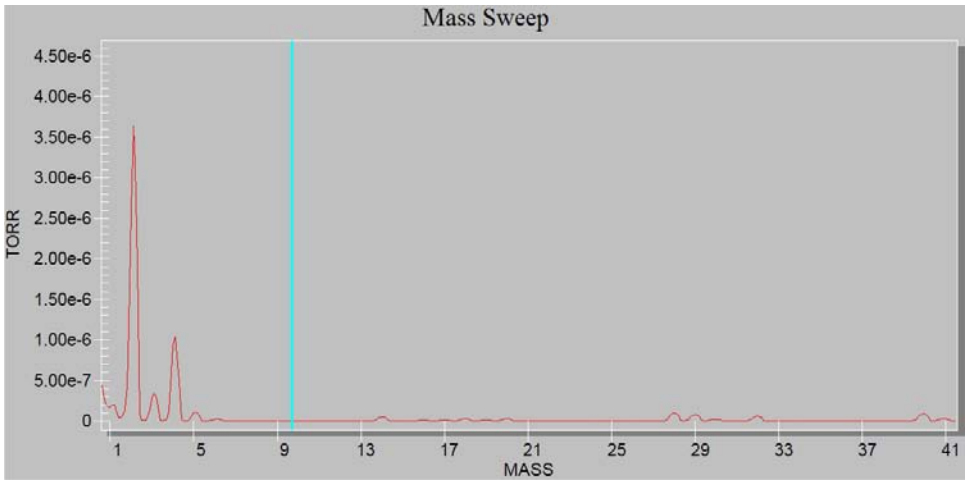

Figure 4.18 During loading the RGA was used to sample the mixed hydrogen-deuterium atmosphere. Note that the Mass 4 peak is much lower than the mass 2 peak, even though the same volume of each was added to the system.

Although equal volumes of hydrogen and deuterium were added to the system, the mass peak representing deuterium is much smaller than that of hydrogen. There are several

mechanisms at work that can cause this discrepancy. The size of the aperture in the pressure reducer is large compared to the size of a hydrogen molecule, so it can be assumed that both hydrogen and deuterium will be pumped through the reducer at the same rate. However, the turbo-molecular pump has a significantly higher compression ratio at mass 4 than at mass 2. This would cause D_2 to be pumped out of the volume around the RGA at a faster rate than H_2. Although the ionization cross-sections for hydrogen and deuterium are the same, the probability that an ionized D_2 molecule will enter the RGA's quadra-pole accelerator is slightly lower. The probability that a D_2 ion will be collected in the faraday cup is also slightly lower. The combination of these three factors could explain why the H_2 peak is higher than the D_2, despite an equal volume of each gas being added to the system. Despite this, it can be assumed that this baseline reading represents an equal mix of hydrogen and deuterium. Once the atmosphere was sampled, the getter was allowed to absorb the gas until the total pressure was below 0.01 mTorr. At this point the getter was heated and the voltage adjusted until an equilibrium pressure of 5 mTorr was reached. Once equilibrium was reached, the valve to the RGA was opened briefly to collect a sample of the atmosphere for comparison. The getter was then cooled until the pressure was below 0.01 mTorr and the process was repeated for four additional trials.□□

4.3.8.2 Results of the Experiment□□

The mass spectrum, show in Figure 4.19, shows the results of one heating cycle of the getter. The mass spectra from the four other trials were very similar. It is interesting to note that the peak at mass 3 has grown much larger in proportion to masses 2 and 4. This is likely due to the way the getter absorbs the hydrogen and deuterium. The gasses are added and molecular H_2 and D_2. However, these molecules are disassociated on the surface of the getter before the atoms are diffused into the bulk of the material. When the getter is heated and the atoms are desorbed from the bulk and reach the surface, they recombine before escaping into the vacuum. The probability of a hydrogen and deuterium combining to form DH is the same and the probability of forming H_2 and D_2. So, it is likely that the gas mix within the DT-111 will be an equal mixture of T_2, D_2 and DT.□□

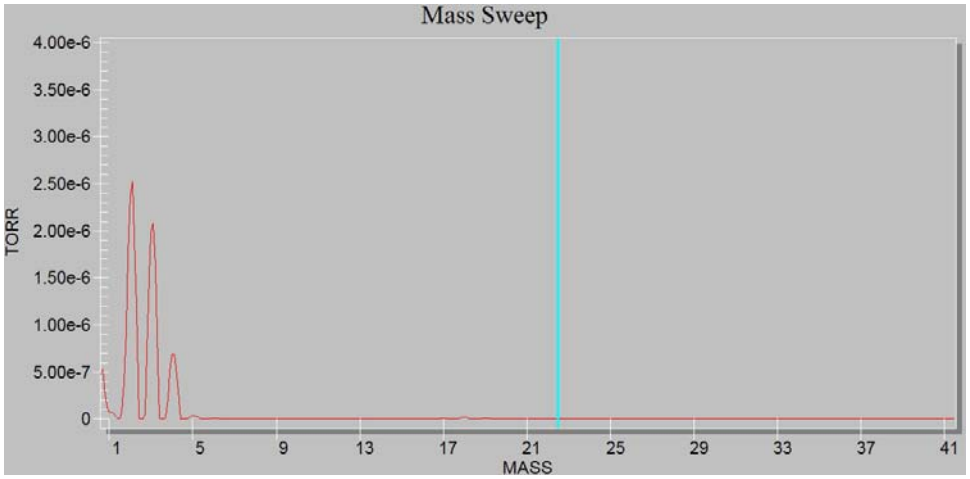

Figure 4.19 The mass spectrum after allowing the getter to absorb H_2 and D_2 and then heating it to release them.

Another lesson of note is the different temperature required to reach a 5 mTorr equilibrium for the two different getters. Some testing is required for each new getter that is constructed to determine the operating voltage required to reach 5 mTorr, due to slight variations in the mass of ST-707 in each one. The stated mass-density of the ST-707 strip is 16 to 24 mg/cm, or 1.6 to 2.4 mg/mm. So, if this quantity is taken as the average mass-density plus or minus some variation, it is d_m =2±0.4 mg/mm. The getter strip is cut into six strips, each 8 mm in length. The length is measured using a steel ruler and cut with a pair of sheers. Assuming each one is cut within 0.1 mm of 8 mm, then the actual length of each is 8±01 mm, so the total length is l=48±0.6 mm. The mass of ST-707 is the product of the length and the mass-density, or $m_g=d_m l$. Through propagation of errors, the mass of ST-707 on the getter can vary by as much as:

$$\sigma\left(m_g\right)=\left[\sigma^2(l)\left(\frac{\partial m_g}{\partial l}\right)^2+\sigma^2\left(d_m\right)\left(\frac{\partial m_g}{\partial d_m}\right)^2\right]^{\frac{1}{2}}. \tag{4.3.3}$$

or,□□

$$\sigma\left(m_g\right)=\left[(0.6\text{ mm})^2(2\text{ mg/mm})^2+(0.4\text{ mg/mm})^2(48\text{ mm})^2\right]^{\frac{1}{2}}=19\text{ mm}. \tag{4.3.4}$$

This seems a small amount, but the volume of gas used in each experiment is very close to the capacity of the getter, so the required temperature to reach 5 mTorr will vary. For instance, while the getter used in the hydrogen only experiment reached 5 mTorr at around 400 °C, the getter used in the two-gas experiment had to be heated to approximately 450 °C.□□

4.3.9 Controlling Gas Pressure with the Getter

The experiment showed that when heat is applied to the getter, the gas pressure increases much more slowly than it decreases when the temperature is reduced. Operationally, this means it is best to heat the getter more than is needed to reach the required pressure, and then slowly lower the voltage until the desired pressure is reached. An operator is required to monitor the pressure within the system and make minute adjustments to the voltage during operation to ensure the same pressure is maintained throughout operation. If the pressure is allowed to fluctuate, the neutron flux will not be constant, and thus it will be difficult to establish repeatability of any experimental results using the DT-111. While a human operator can maintain the pressure to the accuracy of the gauge, it would be beneficial to develop a computer algorithm for monitoring the gas pressure and adjusting the voltage. This would allow faster real-time adjustments and make operation of the prototype more efficient because the user would not have to focus on the pressure.

4.3.10 Recommendations for Further Research

While it can be assumed that the re-designed getter will function as a hydrogen storage and gas pressure control device, there are some possible ways to further increase the understanding of how it operates with two gases. First, it might be beneficial to go back to a one-gas experiment, and add only deuterium to the getter. Care should be taken to ensure that the ratio of hydrogen to mass of ST-707 is the same as in the hydrogen only experiment described above. If a similar equilibrium pressure can be established at a similar temperature to that experiment, then the assumption that the getter handles deuterium in the same manor as it handles hydrogen is further reinforced. It may also be of use to place a valve between the RGA and its associated turbo so that the gas in the main vacuum chamber can be sampled without active pumping. The volume on the RGA side of the pressure reducer could be pumped down to ultra-high vacuum (UHV) conditions, and then this valve closed before opening the valve to allow a gas sample to be taken. The pressure differential between the main chamber and the RGA volume would be sufficient to force a sample through the pressure reducer into the volume around the RGA. The valve between the RGA and main chamber could then be closed. This would eliminate the effects of the different compression ratios of the turbo for different masses.

4.3.11 A Brief Experiment with Titanium as a Getter

With the limited quantity of tritium available for the DT-111, there is some concern that the titanium target may absorb a substantial amount, thus reducing the operating lifetime of the generator. Titanium does have some gettering properties, but is not nearly as strong a gas absorber as the Zr-V-Fe alloys used in the SAES getters. Still, it is prudent to experiment with titanium to ensure that it will not absorb a substantial portion of the available hydrogen gas.

This experiment used the same apparatus as described previously, but the ST-707 getter is replaced with a piece of copper with a layer of titanium brazed onto it, similar to the target configuration. The control volume was pressurized to 5 psi, which is equivalent to 3.2 torr-liters of hydrogen. Once the pressure stabilized, the valve between the titanium and the main chamber was opened. A small drop in pressure is expected given the relatively small increase in volume. If the pressure drops below what is expected, or continues to drop at a steady rate, it can be assumed that the titanium is absorbing the hydrogen. The pressure must be allowed to stabilize, and then the amount of hydrogen absorbed by the titanium can be calculated. When the hydrogen was added to the chamber, the reading on the thermo-couple gauge increased to 475 mTorr. Using the nomogram above, this equates to approximately 300 mTorr in a pure hydrogen atmosphere. When the valve between the titanium and the main chamber was open, the pressure reading dropped to 467 mTorr, the slight drop expected due to the small increase in volume.

After about one hour, the pressure reading was 451 mTorr. There are two mechanisms possibly causing the reduction in pressure. One, the stainless steel walls of the vacuum chamber will trap a small amount of hydrogen on the surface. This is easily confirmed by opening the turbo-molecular pump until the total pressure in the system is below 10^{-7} torr. If the turbo is then closed, the pressure will rise to approximately 10^{-6} torr. Opening the RGA shows a mass peak corresponding to hydrogen, which is out-gassing from the chamber walls under low pressure. The second mechanism is actual absorption in the titanium. Using the current set up, it is impossible to determine which effect is dominant, but it sufficient to note that the percentage of the hydrogen that is absorbed, by both the chamber walls and the target, is small, approximately 3% of the volume added to the system. It should also be noted that the volume of titanium used in this experiment is much larger than that used on the target. So, the absorption of tritium by the titanium target will be negligible compared to the volume stored within the getter.

CHAPTER 5 - Conclusions and Lessons Learned

The SBRS method can provide a rapid and robust method of discerning inert from explosive material. The challenge is in developing a prototype system that is both accurate and safe to operate. Personnel operating the system must be protected from the radiation used to collect signatures from the samples. In order to provide a more accurate system, the neutron flux from the source must be held as close to constant as possible. One way of ensuring constant flux is by carefully controlling the gas pressure within the generator.

5.1 Shielding Concerns

Shielding 14.1 MeV neutrons requires careful design in concert with simulations to ensure adequate shielding. While simulations were used to determine the amount of material required for shielding, care had to be taken in the design of the actual assembly. The volumes of material specified in MCNP were divided into pieces that could be easily manufactured and then assembled. Two-inch thick layers of steel were divided into sheets that are 0.5 inches in thickness. These sheets can be welded together to form the shapes specified by the simulation. The assembly must also be modified to make room for the ancillary components of the DT-111. When placing the DT-111, it is important to ensure that as little shielding as possible is removed to make room. This includes arranging the microwave generator so that it extends along the diagonal of the cube, and running all power and cooling lines through the bottom of the cube to take advantage of the shielding provided by the floor.

5.2 Gas Control Concerns

Deuterium only neutron generators can be operated under active pumping, making gas control a simple matter of using a compressed gas bottle with an adjustable regulator. Any deuterium not used in fusion can be vented to the atmosphere. Deuterium-Tritium (DT) generators cannot be actively pumped because it is not safe to vent radioactive tritium into the atmosphere. SAES getter pumps can be used to control the gas pressure within a DT generator. Hydrogen isotopes can be absorbed by the getter, and then retrieved by applying heat to the alloy. The amount of hydrogen, and its isotopes, that can be retrieved from the getter is a small percentage of what is absorbed. Thus, the getter must be carefully designed so that it is filled to

near capacity with hydrogen. More hydrogen can be retrieved by heating the getter to higher temperatures, but doing so may limit the useful life of the getter.

The getter designed for use in the DT-111 generator is specifically meant to hold 10 Ci of tritium and an equal volume of deuterium. This amount of tritium should be enough to operate the DT-111 for roughly 5700 hours at 10^{11} interactions per second before the neutron flux is significantly degraded from consumption of tritium. If higher intensity or more operating hours are required, a larger getter would need to be designed and a license for more tritium would be required.

Fine-tuning the control of the gas pressure will help ensure a near constant neutron flux. The gas pressure in the reaction chamber is a function of the number of hydrogen atoms within the chamber. Keeping the number of atoms within the chamber stable leads to a stable flux of ions from the ECR source, which in turn leads to a constant reaction rate on the target, and a steady neutron flux. This is important for establishing repeatable results when using the prototype explosive detection system.

CHAPTER 6 - The Way Ahead

After construction of the lab prototype is complete, experimentation can begin in earnest to validate the SBRS method of explosive detection. The library of explosive templates should continue to be expanded. The size and scope of the experiments can be increased to incorporate larger targets and more varied clutter material. The end goal is to have a proven method for discerning explosive from inert material, that can then be applied to a deployable screening system used by military and law enforcement personnel to protect people from harm□□

6.1 Improvements to the Lab Prototype□□

As mentioned in chapter 4, adding computer control and monitoring to the gas pressure will increase the efficiency of the prototype by removing the need for an additional operator to monitor the gas pressure. Ideally, the goal should be to continue developing controls for the neutron source that can automate the entire process so that all an operator needs to do is specify a neutron flux. This would reduce the training required for new operators and increase the speed at which a system could be fielded. □In additional, a control loop monitored electronically several times a second would□enable a more constant neutron flux. A steady neutron flux is crucial for establishing repeatability with the SBRS method.

6.2 Other uses for the SBRS Method□□

Once proven, the SBRS method has numerous applications outside of explosives detection. It can be applied to screening for other controlled substances, such as illegal drugs. A larger scale system could be developed for screening shipping containers quickly and efficiently to increase security at ports.

References

Atzeni, Stefano and Jurgen Meyer-Ter-Vehn . *The Physics of Inertial Fusion: Beam Plasma Interaction, Hydrodynamics, Dense Plasma Physics*. Oxfor University Press Great Calrenton Street Oxford OX2 6DP, 2004. 42

Campbell, Jason H and Michael E. O'Hanlon. *Iraq Index Tracking Variables of Reconstruction & Security in Post-Saddam Iraq*. The Brookings Institute 1775 Massachusetts Ave NW Washington, DC 20036, 2007.

Derenchuk, Vladimir P. "A continuous wave microwave proton source and low energy beam transport for the IUCF cyclotrons". Review of Scientific Instruments, 75:1851–1853, 2004.

Dunn, W.L., R. Brewer, K. Loscke, and J. Lowery, "Radiation Interrogation Using Signature Analysis for Detection of Chemical Explosives". Proc. IEEE Conf. on Technologies for Homeland Security: Enhancing Critical Infrastructure Dependability, Woburn, MA, 16-17 May 2007, pp 7-12.

Ferrario, B., F. Doni, C. Boffito and L. Rosai. "Zr Based Gettering for Hydrogen Isotopes Handling". In 13th Symposium on Fusion Technology, 1984.

Hahto, S., J.H. Vianionpaa, T. Klavas and J. Reijonen. "Experiments with planar inductive ion source meant for creation of h+ beams". Review of Scientific Instruments, 78:1063–1067, 2007.

Hannum, D.W. and J.E. Parmeter. "Survey of Commercially Available Explosive Detection Techniques and Equipment". National Institute of Justice, NCJ 171133, U.S. Department of Justice. 1998

Hoff, M., J.W. Kwan, B.A. Ludewigt, M.J. Regis, J.G. Wallig, R.Wells, J.H. Vainionpaa, R. Gough. "Microwave ion source and beam injection for an accelerator-driven neutron source". In Particle Accelerator Conference, 2007.

Johl, Mark. "MCNP simulations for standoff bomb detection using neutron interrogation". Master's thesis, Kansas State university, 2009.

Lewis, E.E.. *Fundamentals of Nuclear Reactor Physics*. Elsevier Inc 30 Corporate Drive, Suite 400 Burlington, MA 01803, 2008.

Liu, C.Z., S.L. Xu, Z.Y. Zhou, S.Z. Luo, X.G. Long, , L.Q. Shi. Kinetics of Hydrogen Uptake for Getter Materials. Vacuum, 75:71–78, 2004.

Lowery, J.D. and W.L. Dunn, "Signature Based Radiation Scanning Using Radiation Interrogation to Detect Explosives". *Appl. Radiat. Isot.* 68, 893-895. 2010

SAES. *Sorb-AC Cartridge Pumps: Mk 5 Series*. Viale Italia, 77, 20020 Lainate, Italy.

Shultis, J. Kenneth and Richard E. Faw. *Radiation Shielding*. American Nuclear Society Inc., La Grange Park, Illinois 60526, 2000.

Shultis, J. Kenneth and Richard E. Faw. *Fundamentals of Nuclear Science and Engineering, 2nd Edition*. CRC Press 6000 Broken Sound Parkway NW, Suite 300 Boca Raton, FL 33487, 2008.

Song, Dong Jiang Zhizong and Jinxinag Yu. "Small Microwave Ion Source for and Ion Implanter". Review of Scientific Instruments, 67:1003–1005, 1996.

Taylor, Terrence and Jozef F. Mouris. "An Advanced High-Current Low-Emittance DC Microwave Proton Source". Nuclear Instruments and Methods in Physics Research, 336:1–5, 1993.

Taylor, Terrence and John S.C. Wills. "A High-Current Low-Emittance DC ECR Proton Source". Nuclear Instruments and Methods in Physics Research, 309:37–42, 1991.

Teledyne Hastings, Hampton, Virginia 23661. C-184A DV-6, May 1974.

Watanabe, Kuniaki, Kenji Ichimura, Naoya Inoue and Toyosaburo Takeuchi. "Absorbtion and Desorbtion of Hydrogen, Deuterium, and Tritium for Zr-V-Fe getters." Japanese Vacuum Science and Technology, 2:1341–1347, 1984.

Appendix A - Details on the Neutron Source Vault

The dimensions of the individual sheets of steel and plastic used to construct the neutron source vault are detailed below. The top row is the inner most layer of the vault.

	ID of Cube at this layer			These are the dimensions of the individual pieces that make up the six sides of each layer of material													
Source Cavity	Inside			Top		Bottom		Front		Back		Left		Right		Source Cavity
Material	L	W	H	W	H	W	H	W	H	W	H	W	H	W	H	Material
Iron	14	14	38	16	16	16	16	14	38	14	38	16	38	16	38	Iron
				18	18	18	18	16	40	16	40	18	40	18	40	
Polyethylene	18	18	42	20	20	20	20	18	42	18	42	20	42	20	42	Polyethylene
				22	22	22	22	20	44	20	44	22	44	22	44	
Iron	22	22	46	24	24	24	24	22	46	22	46	24	46	24	46	Iron
				26	26	26	26	24	48	24	48	26	48	26	48	
Polyethylene	26	26	50	28	28	28	28	26	50	26	50	28	50	28	50	Polyethylene
				30	30	30	30	28	52	28	52	30	52	30	52	
Iron	30	30	54	32	32	32	32	30	54	30	54	32	54	32	54	Iron
				34	34	34	34	32	56	32	56	34	56	34	56	
Polyethylene	34	34	58	36	36	36	36	34	58	34	58	36	58	36	58	Polyethylene
				38	38	38	38	36	60	36	60	38	60	38	60	
Iron	38	38	62	40	40	40	40	38	62	38	62	40	62	40	62	Iron
				42	42	42	42	40	64	40	64	42	64	42	64	
Polyethylene	42	42	66	44	44	44	44	42	66	42	66	44	66	44	66	Polyethylene
				46	46	46	46	44	68	44	68	46	68	46	68	
Iron	46	46	70	48	48	48	48	46	70	46	70	48	70	48	70	Iron
				50	50	50	50	48	72	48	72	50	72	50	72	
Polyethylene	50	50	74	52	52	0	0	50	73	50	73	52	73	52	73	Polyethylene
				54	54	0	0	52	74	52	74	54	74	54	74	
Iron	54	54	78	56	56	0	0	54	75	54	75	56	75	56	75	Iron
				58	58	0	0	56	76	56	76	58	76	58	76	
Borated Polyethylene	58	58	82	60	60	0	0	58	77	58	77	60	77	60	77	Borated Polyethylene
				62	62	0	0	60	78	60	78	62	78	62	78	
Iron	62	62	86	64	64	0	0	62	79	62	79	64	79	64	79	Iron
				66	66	0	0	64	80	64	80	66	80	66	80	
Polyethylene	66	66	90	68	68	0	0	66	81	66	81	68	81	68	81	Polyethylene
				70	70	0	0	68	82	68	82	70	82	70	82	
Polyethylene	70	70	94	72	72	0	0	70	83	70	83	72	83	72	83	Polyethylene
				74	74	0	0	72	84	72	84	74	84	74	84	
Borated Polyethylene	74	74	98	76	76	0	0	74	85	74	85	76	85	76	85	Borated Polyethylene
				78	78	0	0	76	86	76	86	78	86	78	86	
Borated Polyethylene	78	78	102	80	80	0	0	78	87	78	87	80	87	80	87	Borated Polyethylene
				82	82	0	0	80	88	80	88	82	88	82	88	
Borated Polyethylene	82	82	106	84	84	0	0	82	89	82	89	84	89	84	89	Borated Polyethylene
				86	86	0	0	84	90	84	90	86	90	86	90	

Table A.1 This table shows the dimensions of the six sheets that comprise the six sides of each layer of the neutron source shielding. Each row represents one inch of thickness. The rows labeled as steel are actually constructed of two 0.5 inch thick sheets of equal size.

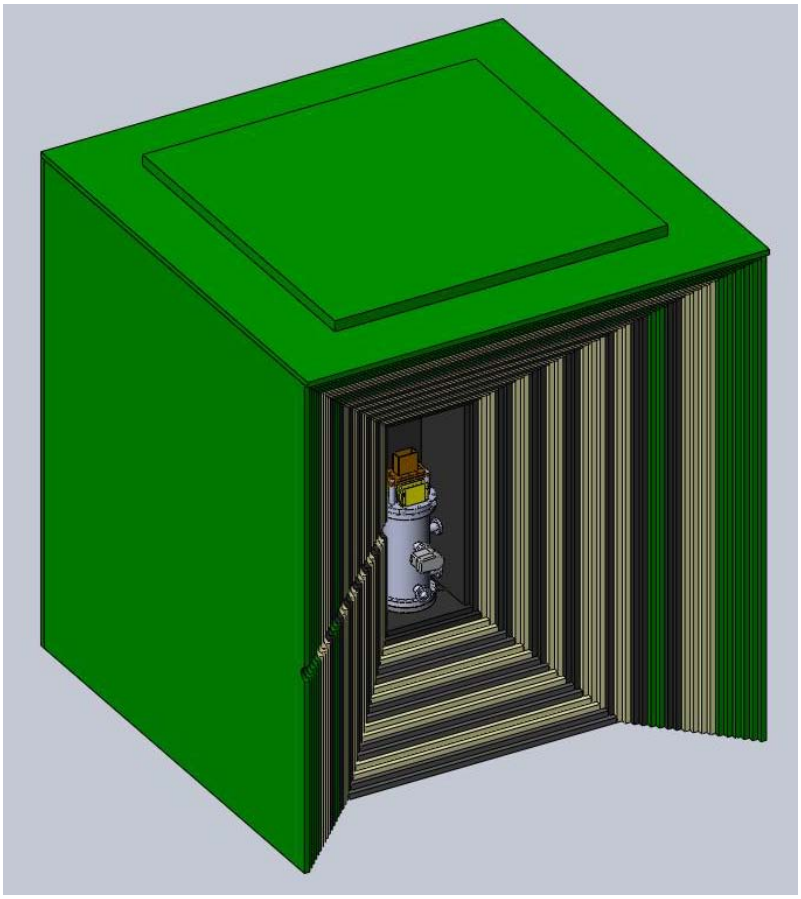

Figure A.1 This isometric view shows the beam port cut away along the diagonal of the source vault.

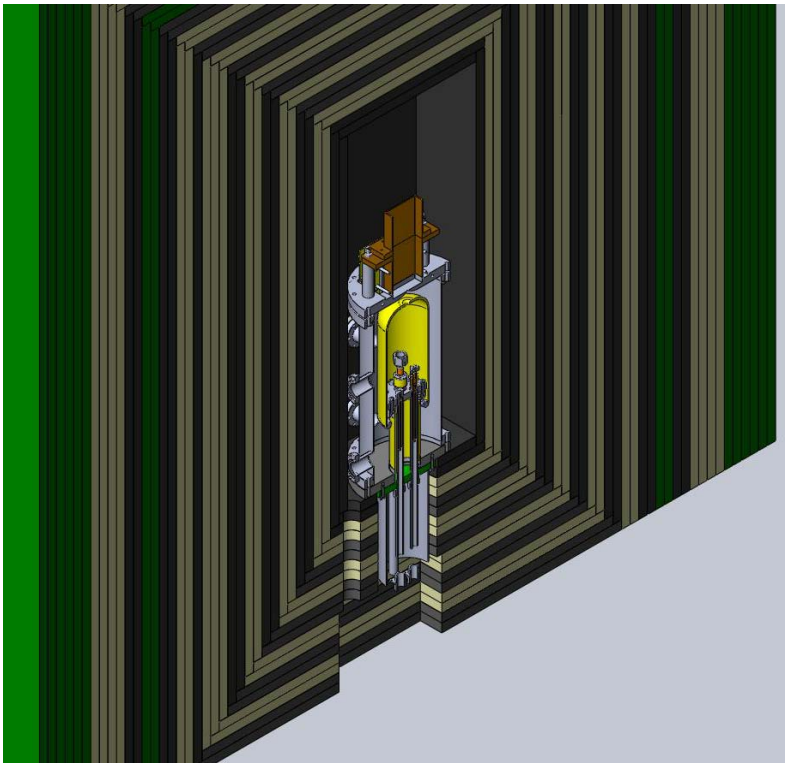

Figure A.2 This close up shows the cut away at the base of the vault for the power and cooling lines for the neutron source.